

**Development of Experimental Setup to Evaluate Drilling Fluid's Characteristic
Using Tomography Method**

by

Norkhairi Bin Muhammad

Dissertation submitted in partial fulfilment of

the requirements for the

Bachelor of Engineering (Hons)

(Mechanical Engineering)

MAY 2011

Universiti Teknologi PETRONAS

Bandar Seri Iskandar

31750 Tronoh

Perak Darul Ridzuan

CERTIFICATION OF APPROVAL

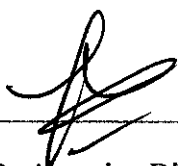
**Development of Experimental Setup to Evaluate Drilling Fluid's Characteristic
Using Tomography Method**

by

Norkhairi Bin Muhammad

A Project dissertation submitted to the
Mechanical Engineering Programme
Universiti Teknologi PETRONAS
in partial fulfilment of the requirement for the
BACHELOR OF ENGINEERING (Hons)
(MECHANICAL ENGINEERING)

Approved by,



(Dr Azuraeni Binti Jaafar)

Project Supervisor

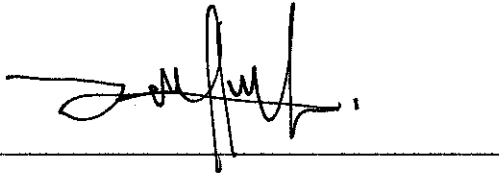
UNIVERSITI TEKNOLOGI PETRONAS

TRONOH, PERAK

May 2011

CERTIFICATION OF ORIGINALITY

This is to certify that I am responsible for the work submitted in this project, that the original work is my own except as specified in the references and acknowledgements, and that the original work contained herein have not been undertaken or done by unspecified sources or persons.

A handwritten signature in black ink, appearing to read 'Norkhairi Bin Muhammad', is written above a horizontal line.

NORKHAIRI BIN MUHAMMAD

ABSTRACT

This report covers the application of drilling fluids and tomography method in the drilling operation. The objectives of the project are to study the characteristics of drilling fluid and to develop new possible testing procedure to evaluate drilling fluid's properties. The literature review describes the drilling fluid additive functions and, current alternatives used focusing on lost circulation and fracture analysis. This report focuses on the Lost Circulation Material (LCM) in drilling fluid. It also confers the methodologies for LCM to resolve severe lost circulation problems and designing the drilling fluid samples, the drilling fluid densities, the rheological tests and the filtration performance volume tests. Tests have been conducted in accordance with the API 13-B and the related equipments are mixer, mud balance, viscometer and high temperature high pressure (HTHP) filters press. Properties measured through this experiment are density, plastic viscosity, yield point and 10-second and 10-minute gel strength. Author has tried to use the equipment available in the Petroleum Department and found out that HTHP filter press equipment for filtration study is not complete for the purpose of evaluating filtration properties of the drilling fluid. The fracture study is included to review the condition of the wellbore when the fracture happen and the solution taken to solve the problem. The study discovered that there is a need to have a new type of testing method in determining the effectiveness of LCM drilling fluid. A experimental rig has been designed and fabricated to evaluate drilling fluid but later discovered that a lot of assumptions have to be made making the rig condition too ideal and unrealistic. The discussion part explained on the results from the calibration and online measurement of the tomography sensor. The preliminary results shows positive signs of correlation between the properties. The conclusion chapter consists of the overall conclusions and recommendations regarding the project. There are a lot more analysis and procedures that can be done in the future to improve the results.

ACKNOWLEDGEMENT

First and foremost, I would like to thank Allah the Almighty who has given me strength and blessings to complete my Final Year Project. The utmost gratitude goes to my supervisor, Dr. Azuraieen bt Jaafar for having her time to guide and assist me in my Final Year Project. Her guidance, support and encouragement have kept the work on the right track with continually motivation. I would also like to give appreciation to Mrs. Nurzharina who has been helping me through many challenges during this project. Moreover, my gratitude goes to all lecturers and lab technologists who had given their help, time, guidance and advice throughout this project. Special thanks to lab technologist Mr. Azhar who assisted me in the laboratory. I would like to use this opportunity to express my deepest appreciation to everyone who has contributed towards this project directly or indirectly. Last but not least, not forgetting my family members and fellow friends who had gave me moral support and motivation.

TABLE OF CONTENT

CERTIFICATION OF APPROVAL	i
CERTIFICATION OF ORIGINALITY	ii
ABSTRACT	iii
ACKNOWLEDGEMENT	iv
LIST OF FIGURES	ix
LIST OF TABLES	xi
CHAPTER 1:									
INTRODUCTION	1
1.1. Background of Study	1
1.2. Problem Statements	2
1.3. Objectives	2
1.4. Scope of Study.	3
CHAPTER 2:									
LITERATURE REVIEW	4
2.1. Drilling Fluid	4
2.1.1 <i>Water Based Drilling Fluid</i>	5
2.1.2 <i>Oil Based Drilling Fluid</i>	6
2.1.3 <i>Synthetic Based Drilling Fluid</i>	6
2.2 Rheological Characteristic	7
2.2.1 <i>Viscosity</i>	7

2.2.2	<i>Gel Strength</i>	8
2.2.3	<i>Yield Point</i>	8
2.2.4	<i>Newtonian Fluid.</i>	8
2.2.5	<i>Non-Newtonian Fluid .</i>	9
2.2.6	<i>Bingham Plastic Model.</i>	10
2.3	Recommended Drilling Fluid Properties	11
2.4	Lost Circulation Material	11
2.5	Formation Type of Losses	12
2.5.1	<i>Naturally Occurring Losses</i>	12
2.5.2	<i>Mechanically Induced Losses.</i>	13
2.6	Severity of Losses	14
2.6.1	<i>Seepage Losses</i>	14
2.6.2	<i>Partial Losses .</i>	15
2.6.3	<i>Severe Losses .</i>	15
2.6.4	<i>Total Losses .</i>	15
2.7	Electrical Resistance Tomography (ERT)	15
2.7.1	<i>Resistance Concept</i>	16
2.7.2	<i>Image Reconstruction of ERT.</i>	17
2.7.3	<i>Measurement Strategies</i>	18
2.7.4	<i>Data Acquisition System</i>	19
2.8	Electrical Capacitance Tomography (ECT)	20

	2.8.1	<i>Capacitance Concept</i>	20
	2.8.2	<i>Number of Electrodes</i>	21
	2.8.3	<i>Length of Electrodes</i>	22
	2.8.4	<i>Earthed Screen</i>	22
	2.8.5	<i>Normalize Capacitance</i>	23
	2.8.6	<i>Image Reconstruction of ECT.</i>	23
	2.9	The Differences between ECT and ERT	24
CHAPTER 3:		METHODOLOGY	26
	3.1	Research Methodology	26
	3.2	Drilling Fluid Base Sample Preparation	27
	3.3	Drilling Fluid Base Sample Weight Measurement	28
	3.4	Drilling Fluid Base Sample Rheology Test	29
	3.5	ERT Sensor Design	30
	3.6	ECT Sensor Design	31
CHAPTER 4:		RESULTS AND DISCUSSION	34
	4.1	Drilling fluid Base Sample Rheology Test	34
	4.2	Filtration Test Rig Design	35
	4.3	Calibration Measurement of ECT Sensor	37
	4.4	Measurement Results	38
	4.5	Discussion	40
CHAPTER 5:		CONCLUSION AND RECOMMENDATION	43

5.1	Conclusion	43
5.2	Recommendation	44
REFERENCES		45
APPENDIX		
	Appendix A: Data Cable	48
	Appendix B: Straight Female Crimp Plug	49
	Appendix C: Copper Foil Shielding Tape.	50
	Appendix D: Industrial Tomography System Device.	51
	Appendix E: Key milestones FYP 1	52
	Appendix F: Gantt Chart	53
	Appendix G: Key milestones FYP 2	54

LIST OF FIGURES

Figure 1:	Diagram Illustrating the Drilling Fluid System . . .	4
Figure 2:	Typical Composition of Water-Based Mud . . .	5
Figure 3:	Typical Composition for Oil-Based Mud . . .	6
Figure 4:	Composition on Synthetic-Based Mud (SARAPAR 147) . . .	7
Figure 5:	Newtonian Fluids Behavior . . .	9
Figure 6:	Non-Newtonian Fluids Behavior . . .	9
Figure 7:	Bingham Plastic Model Plot . . .	10
Figure 8:	Diagram Illustrating the Lost Circulation . . .	12
Figure 9:	ERT Sensor 16 Electrodes Configuration . . .	16
Figure 10:	Example of Schematic Diagram of an ERT System using 4 Electrodes	17
Figure 11:	The structure of a Typical ERT System . . .	17
Figure 12:	Measurement Strategies of ERT . . .	19
Figure 13:	12 Electrodes Arrangement . . .	22
Figure 14:	Project Methodology Process Flow . . .	26
Figure 15:	Multi-Mixer and Mud Balance . . .	28
Figure 16:	Viscometer . . .	30
Figure 17:	Drilling Fluid Base Sample Composition . . .	34
Figure 18:	Filter Press Drilling Fluid Testing Equipment . . .	35

Figure 19:	Design of Test Rig Body	35
Figure 20:	Design of Test Rig Drill String	36
Figure 21:	Design of Test Rig Mud Pusher	36
Figure 22:	Assembly Drawing of Test Rig	36
Figure 23:	Calibration Setup	37
Figure 24:	Low and High Calibration Images	38
Figure 25:	Image of Drilling Fluid Base Sample in Online Measurement		39
Figure 26:	Voltage vs. Electrode Pairs	40

LIST OF TABLES

Table 1:	Empirical Correlations to Determine Upper and Lower Limits of Plastic Viscosity and Yield Point	11
Table 2:	Classification of Loss Severity	14
Table 3:	The Relationship between Number of Electrodes and Number of Independent Measurements	21
Table 4:	Differences between ECT and ERT	25
Table 5:	ERT Sensor Specification for 1 plane.	30
Table 6:	ERT Sensor Fabrication Steps	31
Table 7:	ECT Sensor Specification	32
Table 8:	ECT Sensor Fabrication Steps	32
Table 9:	Properties of Drilling Fluid Base Sample at 10 lb/bbl	34
Table 10:	Voltage Values Measurement.	39

CHAPTER 1

INTRODUCTION

1.1 Background of Study

Drilling fluid was introduced in 1887 where basic mixtures of clays and water that were used had no impact on the surrounding environment. It was first utilized in the period from 1887 to 1901 [Amanullah, 2005]. Throughout this period, the Environmental Protection Agency (EPA) and other regulatory bodies imposed environmental laws and regulations affecting all aspects of petroleum-related operations from exploration, production and refining to distribution [Amanullah, 1993]. Environmental problems associated with complex drilling fluids in general, and oil-based mud (OBM) in particular, are among the major concerns of world communities. For this reason, the EPA and other regulatory bodies are imposing increasingly stringent regulations to ensure the use of environmentally friendly mud and mud additives [Reid, 1993].

Generally, drilling fluid can be classified into two categories; water-based fluids (WBF) and non-aqueous based fluid (NABF). NABF can be divided into subcategories, oil-based mud (OBM), enhanced mineral oil-based mud (EOBM) and synthetic-based mud (SBM). NABF has been used widely because of its superior performance in drilling operations. The performance of OBM has been very good in drilling operation but the high cost and environmental pollution contributed are not desirable. In particular, there has been increasing pressure on exploration companies to find environmentally acceptable alternatives to OBM [Reid, 1993].

The large magnitudes of concerns on the environmental impacts have led to an extensive industrial research to develop an alternative to additives that have the same functions to deliver the same performance. Each additive added to the drilling fluid provides specific function. Among its functions are viscosifiers, weighting agents, pH control, emulsifier, lost circulation material, lubricant, temperature stability agent, and corrosion inhibitor.

Appropriate mixture of additives is vital to ensure its effectiveness besides preserving the marine environment. There are a lot of evaluation techniques to make sure the drilling fluid used in the operation works as the desired plan. The author will fabricate and assess the tomography methods which use Electrical Resistance Tomography (ERT) and Electrical Capacitance Tomography (ECT) sensors in evaluating the drilling fluid's properties.

1.2 Problem Statement

Drilling fluid is an important part in drilling operations. It provides a lot of functions such as controlling the hydrostatic pressure on the borehole wall to prevent uncontrolled flow of reservoir fluids and forms a "filter-cake" on the borehole wall to prevent drilling fluid invasion. To fulfill these tasks efficiently, the drilling fluid contains carefully selected additives to control its chemical and rheological properties. However, in drilling operations, unwanted condition such as fracture does occur.

Fracture in wellbore is unwanted condition during the drilling activity either on onshore or offshore. Generally, the fracture might be happened through three ways. Firstly, the fracture is naturally in the formation even before the drilling activity is started. Secondly, the fracture happened during the drilling activity. It is resulted by overpressure from the drilling fluid pumped into the formation. Thirdly, the fracture happened by the combination of the first and second situations. This condition usually happened during "wild cat" or exploration drilling because of the formation data is inaccurate and also due to the unfamiliar geographical structure. The fracture sizes can vary from 100 microns up to even 5 meters [Baharuddin, 2010]. This resulted in massive lost in circulation and it is one of the most serious and expensive problem in drilling operations.

1.3 Objectives

- To study current drilling fluid rheological behavior used in industry
- To explore the possibility of using tomography method in evaluating lost circulation material in drilling fluid
- To come out with experimental setup to evaluate drilling fluid using tomography method

1.4 Scope of Study

The scope of study consists of the following:

- Literature review
 - Functions of the additives in drilling fluid
 - Current drilling fluid rheological behavior
 - Fracturing study and analysis
 - Tomography methods to evaluate drilling fluid's properties
- Experimental study
 - Formulate and test current drilling fluid properties
 - Test and calibration of tomography sensor

CHAPTER 2

LITERATURE REVIEW

2.1 Drilling Fluid

In geotechnical engineering, drilling fluid is a fluid used to assist drilling boreholes into the earth. It is often used while drilling oil and natural gas wells and on exploration drilling rigs apart from, being used for much simpler boreholes, such as water wells. The mud has a number of functions which must all be optimized to ensure safety and minimum hole problem. Failure of the mud to meet its design functions can prove extremely costly in terms of materials and time, and can also jeopardize the successful completion of the well and may even result in major problems such as stuck pipe, kicks or blowouts [Aminuddin, 2006]. Figure 1 shows a diagram illustrating the drilling fluid system.

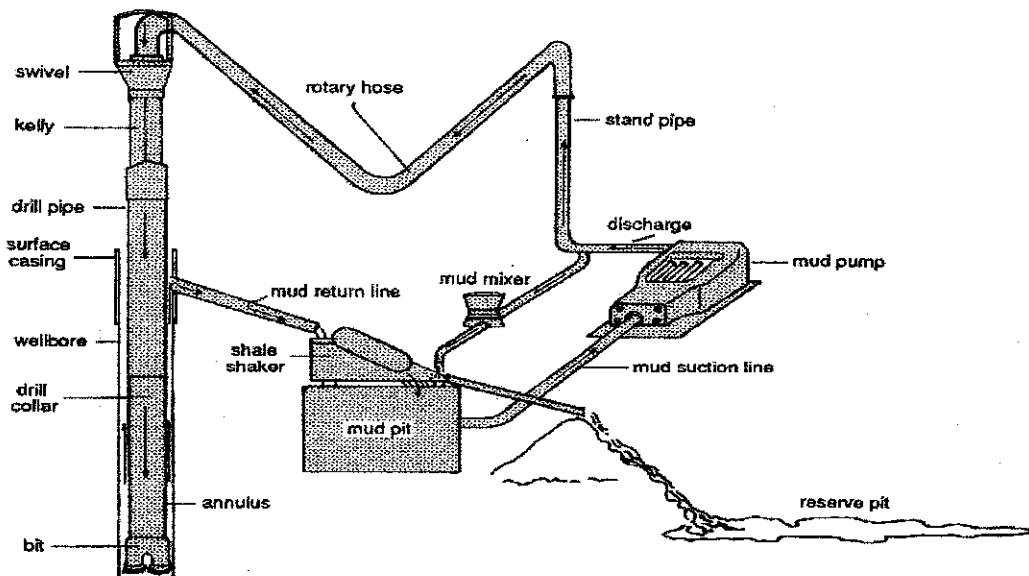


Figure 1: Diagram Illustrating the Drilling Fluid System

The main functions of drilling fluid include providing hydrostatic pressure to prevent formation fluids from entering into the well bore, keeping the drill bit cool and clean during drilling, carrying out drilling cuttings, and suspending the drill cuttings while drilling is stopped and when the drilling assembly is brought in and out of the hole. The drilling fluid used for a particular job is selected to avoid formation damage and to limit corrosion [Liesman, 2000].

2.1.1 Water Based Drilling Fluid

A most basic water-based mud system begins with water, then clays and other chemicals are incorporated into the water to create a homogenous mixture depending on desired viscosity. The clay is usually a combination of native clays that are suspended in the fluid while drilling, or specific types of clay that are processed as additives [Amanullah, 1993]. The most common of these is Bentonite, frequently referred to in the oilfield as “gel”. Many other chemicals are added to a WBM system to achieve various effects, including viscosity control, shale stability, enhance drilling rate of penetration, cooling and lubricating the equipment. Figure 2 shows typical composition of WBM [Azuraie, 2010].

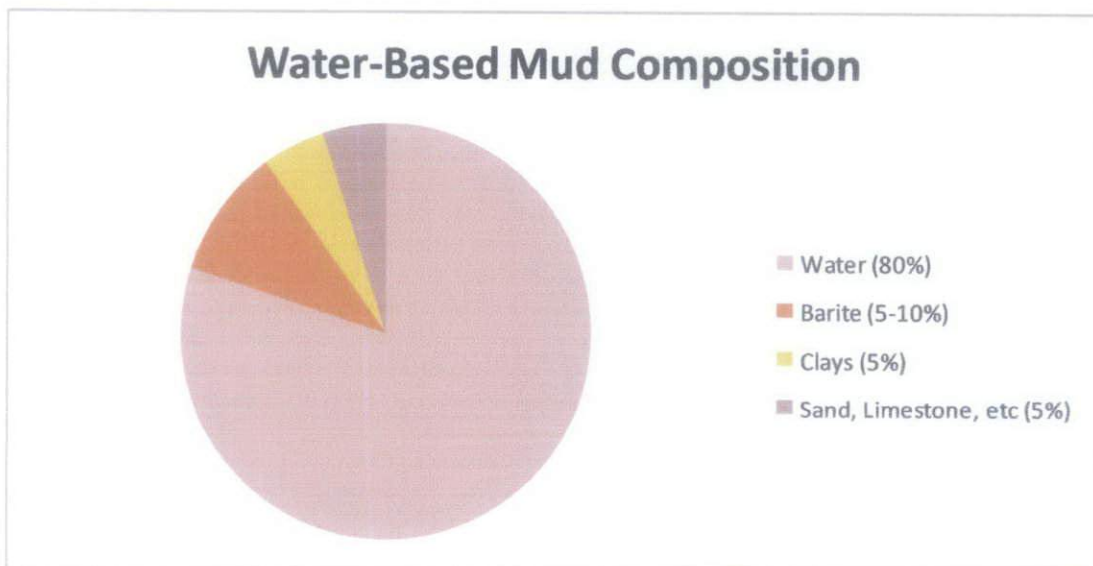


Figure 2: Typical Composition of Water-Based Mud

2.1.2 Oil Based Drilling Fluid

Oil-based mud can be a drilling fluid where the base fluid is a petroleum product such as diesel fuel. Oil based-mud such as diesel has a very good yield point (low yield point) for high rate of penetration (ROP) during drilling and high plastic viscosity for lifting up drilling cuttings. Hence, oil-based mud systems are usually applied when drilling sensitive production zones, drilling salt section and formation that contains hydrogen sulfide [Aminuddin, 2006]. However, the use of oil-based mud has special considerations. These include high cost and requires environmental pollution consideration. Figure 3 shows typical composition of OBM [Azuraian, 2010].

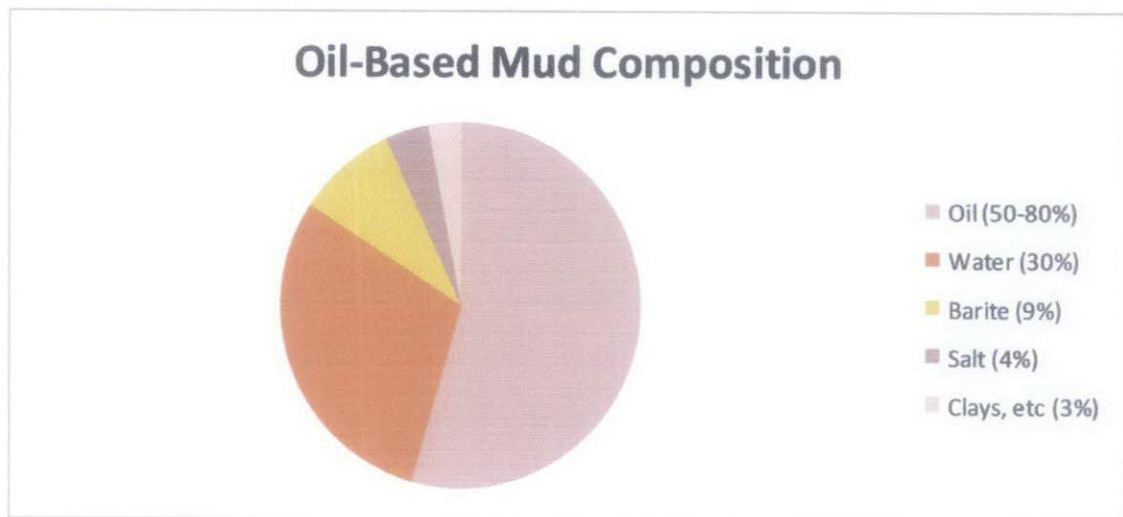


Figure 3: Typical Composition for Oil-Based Mud

2.1.3 Synthetic Based Drilling Fluid

Synthetic-based fluid is a drilling fluid where the base fluid is synthetic oil. Nowadays, SBF is often being used on offshore rigs because it has the properties of an oil-based mud with the toxicity of the fluid fumes to be much less than an oil-based fluid [Oil Glossary]. Synthetic-based fluid has been developed to meet difficult drilling targets with reduced environmental impact [McKee, 1995]. In Malaysia for example, current environmental regulations prohibit discharge of OBM or any oil mud cutting to the sea that will cause

marine pollution and hence, SBM would be of advantage [Liesman, 2000]. Figure 4 shows the composition of SBM [McKee, 1995].

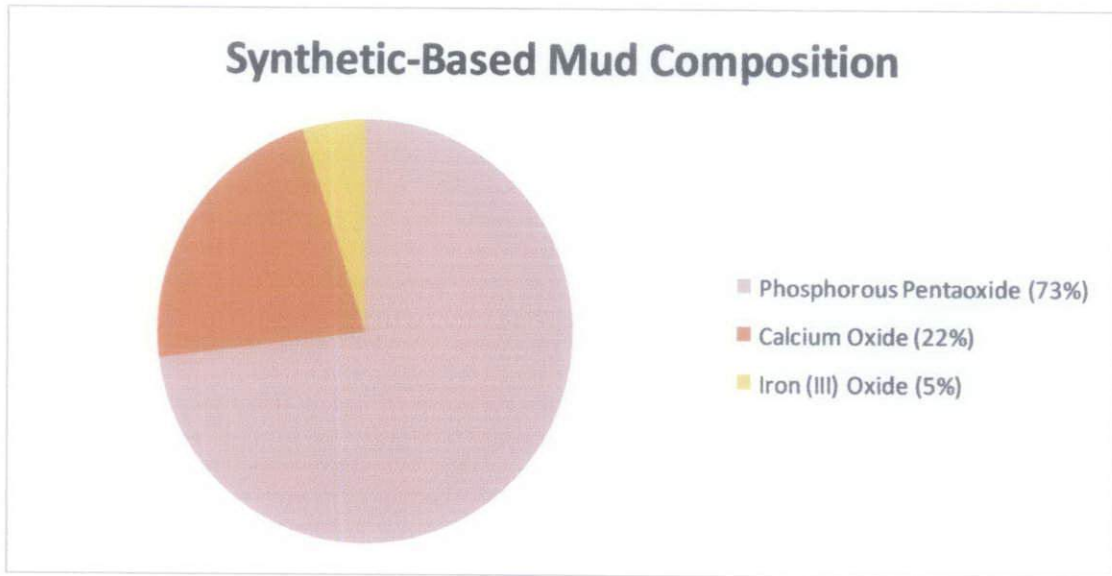


Figure 4: Composition on Synthetic-Based Mud (SARAPAR 147)

2.2 Rheological Characteristic

Basic properties of drilling fluid are its density (weight), plastic viscosity, gel strength, yield point, pH value and its filtration properties. The effectiveness of the drilling fluid in performing its functions is directly related to these properties. Drilling fluid properties are measured on a continual basis while drilling and adjusted with additives or dilution to meet the needs of the operation. Determining what adjustments need to be made to give the desired properties is very important. There are two types of fluid: Newtonian fluid and non-Newtonian fluid. Most of drilling fluids are non-Newtonian fluid [Van Dyke, 1951].

2.2.1 Viscosity

The viscosity of a drilling fluid is its resistance to flow. A drilling fluid with high viscosity resists flow more than a drilling fluid with low viscosity. A simple example is honey with high viscosity and exhibits high resistance to flow more than water which has low viscosity. A viscous drilling fluid can transport more and heavier cuttings, so drilling fluid often contains a material or additives to increase its viscosity. However, the

viscosity also must be controlled. A drilling fluid is which too viscous gives too much strain on the mud pump and may interfere with other desirable drilling fluid properties required to drill the well efficiently [Van Dyke, 1951].

2.2.2 Gel Strength

Gel strength is a measure of the drilling fluid's ability to suspend the drill cuttings. An additive is added to drilling fluid when circulation stop to make the drilling fluid became gel or stiffen to avoid the drill cuttings going down to the bottom of boreholes. When the mud pump start again, pump pressure un-gel the mud and it flows normally. Bentonite is a good additive to increase gel strength, it is a special clay that not only builds the gel strength, but also viscosity. Gel strength is also still needed to be controlled because too high a gel strength may require high pump pressure to restore the flow after circulation break [Van Dyke, 1951].

2.2.3 Yield Point

The drilling fluid's yield point is a measure of the force required to start the flow. The attraction between clay particles in the drilling fluid affected the amount of force required to start up the flow. This attraction causes the particles to flocculate (get-together). This flocculate can be desirable or otherwise, and it also may be the result from either additives or contaminated. A thinner can be used to deflocculate a contaminated drilling fluid while flocculating agent is used to increase flocculation or thicken the drilling fluid [Van Dyke, 1951].

2.2.4 Newtonian Fluid

Newtonian fluid has a constant viscosity at all shear rates at a constant temperature and pressure. The shear stress of Newtonian fluid is directly proportional to the shear rates. An equation describing a Newtonian fluid is:

$$\mu = \tau / \gamma \quad \text{eq. (1)}$$

where,

$$\mu = \text{viscosity}$$

τ = shear stress

$\dot{\gamma}$ = shear rate

The equation is called Newton's Law of viscosity. Water, sugar solutions, glycerin, silicone oils, light-hydrocarbon oils, air and other gases are examples of Newtonian fluid.

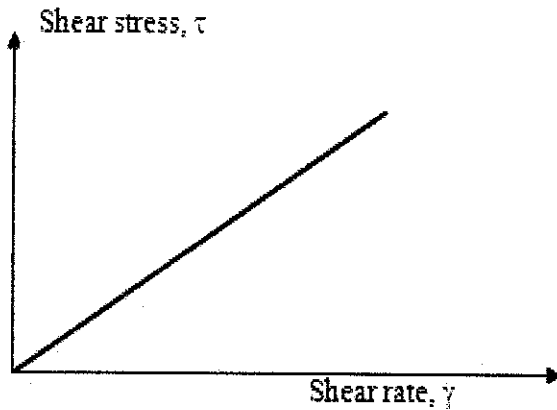


Figure 5: Newtonian Fluids Behavior

Referring to the Figure 5, a straight line passing through the origin; the fluid begins to move with less force compare to solid [Technip, 1982].

2.2.5 Non-Newtonian Fluid

Non-Newtonian fluid are fluid which has no direct proportionality between shear stress and shear rate. The figure below shows one example of a non-Newtonian fluid. For such fluid a certain stress must be applied first (τ_0) to initiate flow. This fluid is classified as a yield stress fluid which can be described by Bingham Plastic model.

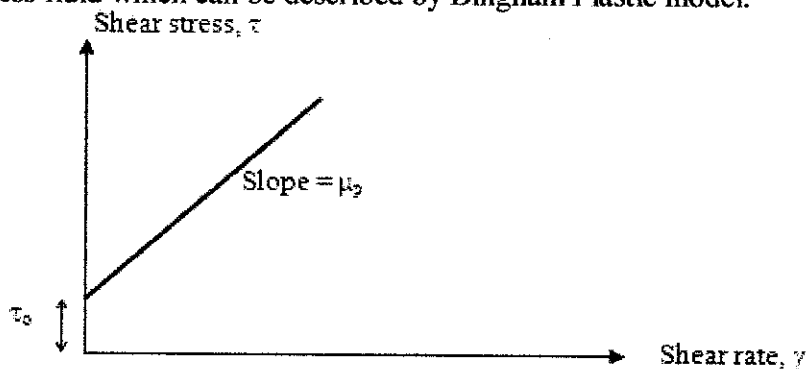


Figure 6: Non-Newtonian Fluids Behavior

For non-Newtonian fluid, the viscosity varies with the shear rate. Most drilling fluid is non-Newtonian and varies considerably in their flow behavior. To be significant, a viscosity measurement made on a non-Newtonian must always specify the shear rate. Drilling fluid are shear thinning when they have reduced viscosity at higher shear rates than at a lower shear rate [Technip, 1982].

2.2.6 Bingham Plastic Model

Bingham plastic model is a two-parameter rheological model used in the drilling fluids industry to describe flow characteristics of many type of drilling fluid. An equation describing a Bingham plastic fluid is:

$$\tau = YP + PV (\dot{\gamma}) \quad \text{eq. (2)}$$

where,

- τ = shear stress
- $\dot{\gamma}$ = shear rate
- YP = yield point
- PV = plastic viscosity

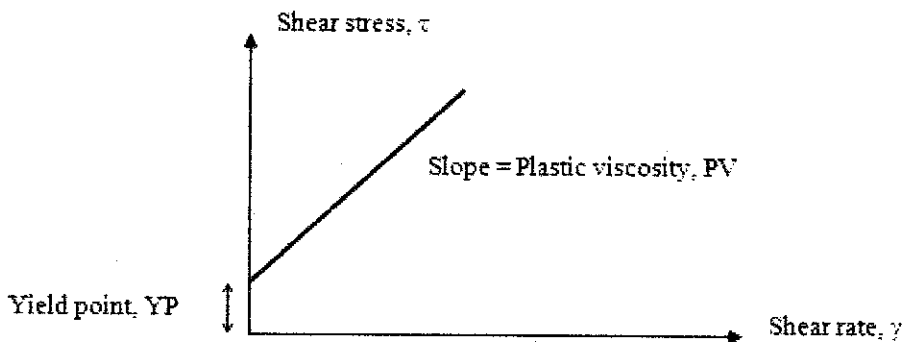


Figure 7: Bingham Plastic Model Plot

Fluids obeying this model which demonstrate a linear shear-stress, shear-rate behavior after an initial shear stress threshold has been reached is called Bingham plastic fluid. Plastic Viscosity (PV) is the slope of the line while Yield Point (YP) is the threshold stress. PV should be as low as possible for fast drilling and is best achieved by minimizing colloidal solids. YP must be high enough to carry cuttings out of the hole, but

no so large as to create excessive pump pressure when starting the drilling fluid flow. YP is adjusted by careful choices of the drilling fluid treatments [Technip, 1982].

2.3 Recommended Drilling Fluid Properties

The empirical correlations are used to compute the recommended upper and lower limits of the plastic viscosity and the yield point which is shown in the following figure. All the correlations below are based on the drilling fluid density and suitable for all types of fluids.

Table 1: Empirical Correlations to Determine Upper and Lower Limits of Plastic Viscosity and Yield Point

Acceptable Plastic Viscosity Range		
Mud Weight (ppg) Range	Plastic Viscosity (cP)	
	High range	Low Range
$\rho_m < 14$	$3.40 \rho_m - 18.6$	$2 \rho_m - 14$
$14 \leq \rho_m < 17$	$5 \rho_m - 40$	$4.33 \rho_m - 46.95$
$17 \leq \rho_m < 18.4$	$8.57 \rho_m - 100.25$	$8.57 \rho_m - 118.25$
$\rho_m \geq 18.4$	$16.68 \rho_m - 248.73$	$16.67 \rho_m - 266.73$

Acceptable Yield Point Range		
Mud Weight (ppg) Range	Yield Point, (lb/ft²)	
	High Range	Low Range
$\rho_m < 11$	$-4 \rho_m + 66$	$0.4 \rho_m - 0.6$
$11 \leq \rho_m < 14$	$-1.67 \rho_m + 40.04$	$0.4 \rho_m - 0.6$
$\rho_m \geq 14$	$-0.6 \rho_m + 25.4$	$0.4 \rho_m - 0.6$

Source: [Drilling Eng. Manual, Curtin University]

2.4 Lost Circulation Material

Lost circulation is defined as the total loss of drilling fluids into the formation. It also refers to the drilling fluid that is lost to formation or by other mean, where parts or all of the circulating drilling fluid fails to return to the surface. The lost drilling fluid might get into faults or fractures in the formation or into gravel beds that the drilling exposed in the

hole. Lost circulation is one of the most serious and expensive problems in drilling. To solve this problem, certain materials or additives can be added into the drilling fluid that will seal fractures by plugging them. Lost circulation material come in variety of shape and sizes: they consist of grains, flakes, or fibers and can be coarse, medium, or fine [Van Dyke, 1951].

For this to occur both of the following conditions must exist:

- The drilling fluid overbalances the problem formation.
- There is a path that allows the mud to flow into the formation and away from the wellbore.

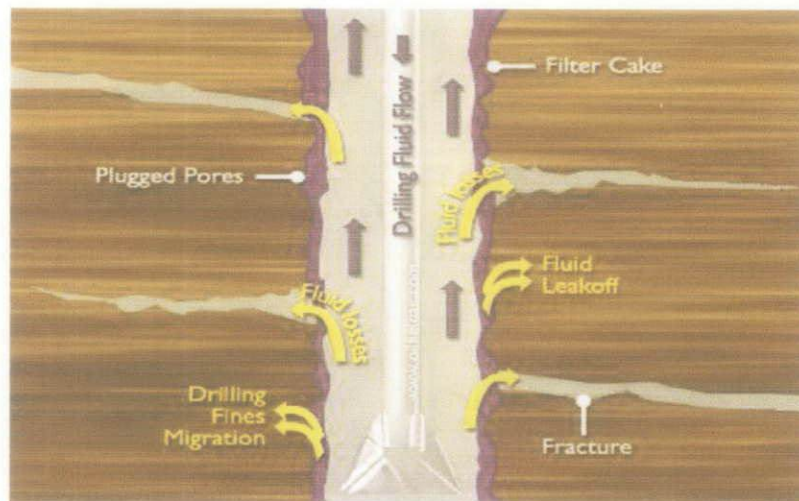


Figure 8: Diagram Illustrating the Lost Circulation

2.5 Formation Type of Losses

Lost circulation of differing intensity can occur at any depth in various formations. In order to precisely and accurately define the situation on the rig, the type and volume of losses must be identified and classified. The type of losses can generally be classed as one of the following:

2.5.1 Naturally Occurring Losses

Naturally occurring losses can be defined as losses resulting from some aspect of the formation being drilled. Losses are common in various formations such as:

- Unconsolidated formations which include sand and gravel.
- Permeable formations such as poorly cemented sandstone.
- Cavernous and vugular formations which include gravel, limestone and dolomite.
- Natural fractures or fissures which can occur at all depths and in all formations. Losses increase in older, harder more consolidated formations with depth. It is common to encounter fractures near faults and areas exposed to tectonic stress. Voids and fractures can generally be recognized by a change in the drilling parameters and when this occurs losses can be expected.

Commonly, when losses occur whilst drilling these formations, they will increase proportionally with depth as more of the formation is exposed. Invariably LCM treatment of some degree, and associated lost time, is required to minimize or cure these losses [Zairul Zahha, 2011].

2.5.2 Mechanically Induced Losses

Mechanically induced losses can be defined as losses resulting from some aspect directly related to the drilling operation. Losses are caused by over pressuring and fracturing the formation which, once fractured, will easily re-fracture with over pressure. The most common causes of mechanically induced losses are:

- High hydrostatic pressure resulting from an excessive mud weight.
- High hydrostatic pressure resulting from an excessive annular cuttings load.
- High hydrostatic pressure resulting from an excessive Equivalent Circulating Density (ECD).
- High surge pressure resulting from an excessive drill string or casing running speed.
- High downhole pressure resulting from a restricted annulus.

Commonly, when losses are induced, they can be minimized or cured by altering the drilling or operational parameters without resort to loss circulation treatment [Zairul Zahha, 2011].

2.6 Severity of Losses

Lost circulation occurs in varying degrees and the severity of these losses is an indicator of the mud loss to the formation. It can arbitrarily be classed as one of the following:

Table 2 : Classification of Loss Severity (Scomi 2010)

Seepage losses	< 10	< 1.59
Partial losses	10 – 30	1.59 – 4.77
Severe losses	30 – 100	4.77 – 15.9
Total losses	> 100	> 15.9

2.6.1 Seepage Losses

Seepage losses are arbitrarily defined to as dynamic losses of up to 10 bbl per hour when circulating at the minimum pump rate used for drilling. Static losses are generally not associated with this classification. Commonly, initial seepage losses will be minimal and will increase with drilling as more of the specific formation is exposed. Losses of this severity are commonly encountered in porous sands and fractured formations.

The type of loss, naturally occurring or mechanically induced, can usually be resolved by suspending drilling, circulating the hole clean and observing the losses whilst varying the pump rate and pressure. It is not uncommon for seepage losses to self heal with time as cuttings bridge the pore throats or micro fractures [Zairul Zahha, 2011].

2.6.2 Partial Losses

Partial losses are arbitrarily defined as dynamic losses of 10 – 30 bbl per hour when circulating at the minimum pump rate used for drilling. Static losses are sometimes associated with this classification. Losses of this severity are commonly encountered in unconsolidated formations, vugular carbonates and fractured formations.

The type of loss, naturally occurring or mechanically induced, can usually be resolved by suspending drilling, circulating the hole clean and observing the losses whilst varying the pump rate and pressure.

2.6.3 Severe Losses

Severe losses are arbitrarily defined as dynamic losses of more than 30 - 100 bbl per hour when circulating at the minimum pump rate used for drilling. Static losses are generally associated with this classification. Commonly, severe losses are instantaneous as fluid is lost to a void, the initial volume lost can range from tens to hundreds of barrels after which the losses may moderate or cease. Losses of this severity are commonly encountered in vugular carbonates and fractured formations. The type of loss can be assumed to be naturally occurring [Zairul Zahha, 2011].

2.6.4 Total Losses

Total losses are arbitrarily defined as a total absence of returns when circulating at the minimum pump rate used for drilling. Static losses are also very high which necessitates new mud volume with which to maintain a full annulus. Commonly, it is often difficult, if not impossible, to mix new mud volume at the rate required to maintain a full annulus with high static losses, such a situation may result in a well control situation as the mud column and resultant hydrostatic pressure is diminished [Zairul Zahha, 2011].

2.7 Electrical Resistance Tomography (ERT)

Tomography involves taking measurements around the periphery of an object, for example vessel or patient, to determine the flow behavior within. There are several tomography techniques that involve the measurement of electrical properties such as

electrical resistance tomography (ERT), electrical capacitance tomography (ECT) and electromagnetic tomography (EMT). In this project, ERT and ECT are explored where it involves the measurement of fluid resistance and capacitance.

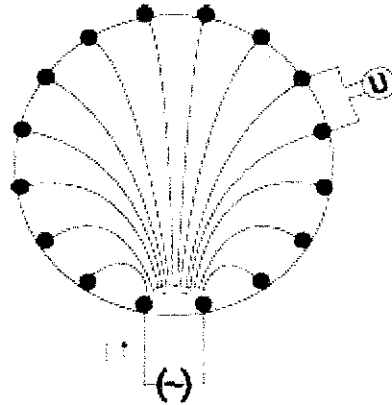


Figure 9 : ERT Sensor 16 Electrodes Configuration

2.7.1 Resistance Concept

An ERT system produces a cross-sectional image showing the distribution of electrical conductivity of the contents of a process vessel or pipeline from measurements taking at the boundary of the vessel. Basically, the operating principle of ERT is that the systems will inject a current between a pair of electrodes and the resultant voltage difference between remaining electrodes pairs will be measured according to a pre-defined measurements protocol. Based on the resistance data, the material distribution can be obtained using sensitivity maps or physical models of the sensor arrangement.

Figure 10 shows a schematic diagram of an electrical resistance tomography system. The apparent electrical conductivity is calculated as the ratio of the applied current to the measured potential, with a correction applied for the geometrical effects of the electrode spacing. This apparent electrical conductivity is some weighted average of the electrical conductivities of the subsurface regions through which current flows.

However, an infinite number of electrical conductivity distributions can give rise to the same apparent electrical conductivity. To resolve this non-uniqueness problem, a large

number of overlapping measurements are made and interpreted simultaneously [Telford, 1990].

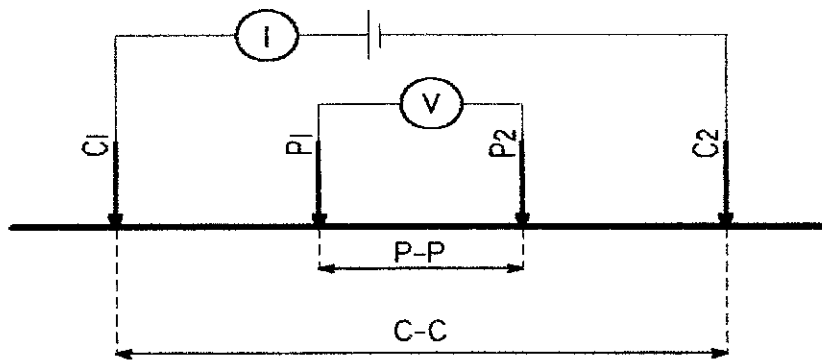


Figure 10: Example of Schematic Diagram of an ERT System using 4 Electrodes

In an ERT system, the electrodes are directly in contact with the material inside the vessel. The structure of a typical ERT system is composed of three main parts: sensor, data acquisition system and image reconstruction system/host computer (see figure 11).

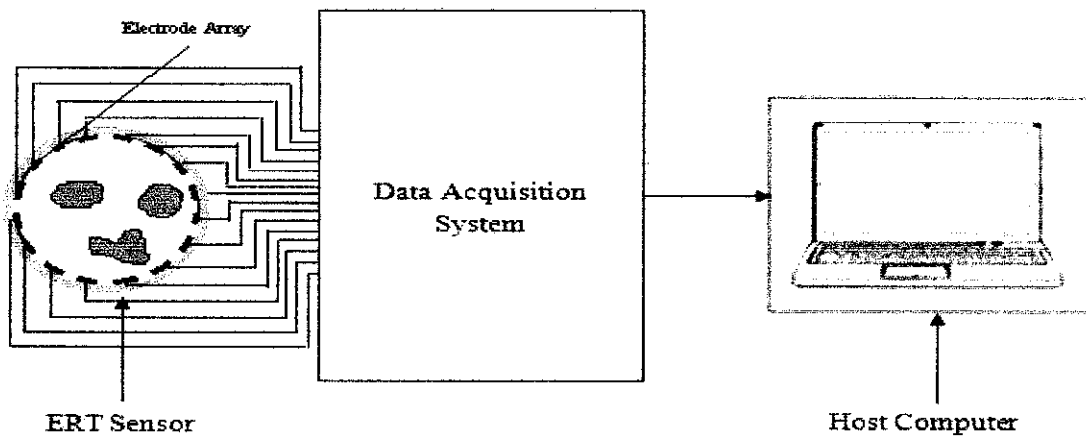


Figure 11: The structure of a Typical ERT System

2.7.2 Image Reconstruction of ERT

The goal of image reconstruction in ERT is to compute a tomogram representing the electrical conductivity of material flowing within the sensor from voltages measured at the periphery of the sensor in response to the injected electrical current. A number of methods can be used to reconstruct the image, for example ridge-regression, Newton-Raphson method (non-linear iterative scheme), back-projection scheme, etc.

The linear back-projection (LBP) algorithm is used because it is very simple and computationally fast, due to the fact that the reconstruction process is reduced to matrix-vector multiplication.

Over the years, many image reconstruction techniques have been proposed for electrical tomography, but the simplest one, the LBP is still the most widely used because it allows online imaging. The excellent time resolution and the qualitative images provided by LBP are often sufficient to monitor and visualize transient multiphase flows [R. Giguere, 2007]. In LBP algorithm, the potential difference is calculated by the forward solver, between two equipotential on the boundary that was back-projected to a resistivity value in the area enclosed by the two lines for all possible injection/measurement combinations [F. L. Quak, 2008].

LBP gives the relative difference between the conductivity distributions in the test set and that of a single reference set. The algorithm assumes that no sharp conductivity differences exist in the measurement plane and smoothers interfaces where severe conductivity gradients exist.

Nonetheless, this direct method is based on making a linear approximation to a problem that is essentially non-linear. Therefore, it causes considerable errors, which are significant particularly if there are large conductivity differences in the image.

2.7.3 Measurement Strategies

Measurement strategies for ERT include normal adjacent, linear and conducting boundary strategies (see figure 12). Normal adjacent is a measurement technique where current is applied through two neighboring electrodes and voltage is measured from the remaining pairs of neighboring electrodes. In this strategy, N^2 measurements are yielded where N is the number of electrodes. To avoid electrodes/electrolyte contact impedance problems, the voltage is not measured at a current injecting electrode and the total number of independent measurements M is reduced to $N(N-3)/2$.

This adjacent strategy is the recommended measurement strategy for sensors with insulating boundaries with electrodes arranged at equal intervals around the periphery of

the sensor [F. L. Quak, 2008]. Fast adjacent is a measurement which is only suitable for fast data collection when no on-line image processing is performed. The principles are the same as those described for the normal adjacent strategy.

Other measurement strategy is linear measurement. It is used when a vertical series of electrodes mounted either on a linear rod or fixed along the inside of a vessel [F. L. Quak, 2008]. Whereas, conducting boundary strategy is a measurement applied to pipelines and vessels with conducting boundaries. For example, stainless steel pipes.

The relatively large surface area of the conducting boundary is employed as the current sink to reduce the common-mode voltage across the measurement electrodes. The earthed conducting boundary also acts as shield, reducing the effects of the electromagnetic interference [F. L. Quak, 2008].

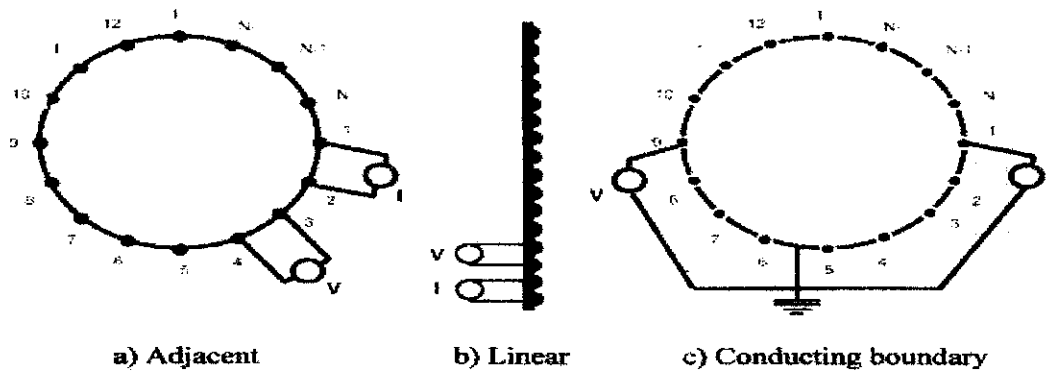


Figure 12: Measurement Strategies of ERT

2.7.4 Data Acquisition System

The Data Acquisition System (DAS) is responsible for obtaining the quantitative data describing the state of the conductivity distribution inside the vessel. The data must be collected quickly and accurately in order to track small changes of conductivity in real-time thus allowing the image reconstruction algorithm to provide an accurate measurements of the true conductivity distribution [F. L. Quak, 2008]. A sine-wave voltage output is fed into voltage-to-current converter (referred to as a voltage controlled current sources- VCCS). Current is used in preference to voltage as the electrical ‘probe’ due to the variation of contact impedance between electrodes and the fluid inside the

sensor. The VCCS circuit maintains constant output current amplitude over a wide range of resistance leads by employing two operating amplifiers and an analogous switch arrangement in the feedback path of one of the operational amplifier (op-amps). The DAS communicates with the host computer via a fast bi-directional RS232 serial link to receive logging commands and to transfer logged data for subsequent image reconstruction.

2.8 Electrical Capacitance Tomography (ECT)

In ECT the changes in inter-electrode capacitance due to the change in concentration and/or distribution of dielectric materials in the region are measured, and a cross-sectional image representing the permittivity distribution inside a pipe or vessel is reconstructed [S. M. Huang, 1992]. ECT measures the capacitance between electrode pairs, captures and converts the measurement data into an image permittivity distribution through data acquisition system.

2.8.1 Capacitance Concept

Capacitance is the main component that harnesses electric charge which has essentially a pair of conductors containing moveable electric charge separated by a dielectric or insulator. A capacitor is formed when any two conducting bodies (regardless of the shapes and sizes) separated by an insulating medium [F. Ulaby, 2005]. Capacitance can be defined as the magnitude of charges, Q on both electrodes divided by the potential difference between electrodes, V . The voltage supply will transport charge from one plate to the other until the voltage produced by the charge build up is equal to the voltage supply. Capacitance is typified by a parallel plate arrangement and is defines in terms of charge storage :

$$C = Q/V \quad \text{eq. (3)}$$

where,

Q = magnitude of charge stored on each plate

V = voltage applied to the plates

2.8.2 Number of Electrodes

The first step to design an ECT is deciding the number of electrodes on the sensor. With small number of electrodes, the expected benefits are a smaller number of data acquisition channels are required, a faster data acquisition rate as the number of capacitance measurement is reduced, and the length of electrodes may be reduced due to the increased cover angle of the electrodes resulting in increased inter-electrode capacitance. However, with a small number of electrodes, the number of independent capacitance measurements is small and therefore a good image cannot be expected [W. Q. Yang, 2010].

The basic method is to surround the vessel or pipe with a set of electrodes (metal plates) and take capacitance measurements between each unique pair of electrodes [Process Tomography Ltd, 2004]. The number of independent capacitance measurements can be calculated by $N(N-1)/2$, where N is the number of electrodes. Based on the number of independent capacitance measurements equation, there are 66 independent capacitance measurements for 12 electrodes ECT sensor. Example of twelve electrodes arrangement is shown in Figure 13.

Table 3: The Relationship between Number of Electrodes and Number of Independent Measurements

No. of electrodes	No. of independent measurement	Typical speed (frames s ⁻¹)	Application example	References
6	15	400	Visualizing combustion flame in an engine cylinder with to achieve 36000 frames s ⁻¹	Waterfall <i>et al.</i> (1996)
8	28	200	Imaging a wet gas separator.	Yang <i>et al.</i> (2004)
12	66	100	Measuring gas-oil-water three-component flows.	Yang <i>et al.</i> (1995)
16	120	50	Imaging the nylon polymerization process.	Dyakowski <i>et al.</i> (1999)

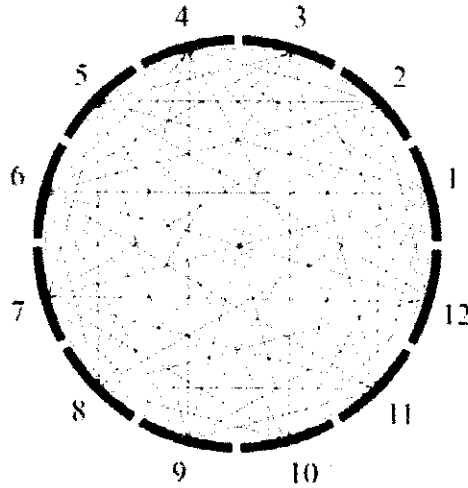


Figure 13: 12 Electrodes Arrangement

2.8.3 Length of Electrodes

Although smaller and larger ECT was attempted, the diameter of an ECT sensor is usually between 1 and 4 inches (between ~2.5cm and ~10cm) [W. Q. Yang, 2010]. Typically, the length of electrodes is larger than the diameter of the insulating pipe so that a serious fringe effect at both end axial can be avoided.

2.8.4 Earthed Screen

The function of the earthed screen is to prevent interferences between the sensor's applied signal and any devices present near the capacitance sensor. The electrodes are used to initiate the charge and detect capacitance between two electrodes. The insulation guard function is to reduce stray capacitance between back surfaces of adjacent electrodes. There are three type of earthed screens may be used in an ECT sensor which are an outer screen, two axial end screens, and radial screens. It is crucial to use an earthed outer screen to prevent interference of external noise [W. Q. Yang, 2010]. It is common to use two earthed axial end screens at both ends of measurement electrodes which can reduce external noise to some extent [D. A. Robinson, 1998]. The standing capacitance between adjacent electrode pairs can be reduced by using earthed radial screen.

2.8.5 Normalize Capacitance

There are two types of measurement is ECT which are calibration and online measurement. The calibration measurement in lower and higher permittivity material gives lower and higher capacitance (C_l and C_h) values respectively while online measurement gives measured capacitance value, C_m . All subsequent measured capacitance values C_m are then normalized to have values C_n between “0” (when the sensor is fully filled with the lower permittivity material) and “1” (when fully filled with higher permittivity material) according to the equation (4) [W. Q. Yang, 2004]:

$$C_n = \frac{C_m - C_l}{C_h - C_l} \quad \text{eq. (4)}$$

2.8.6 Image Reconstruction of ECT

Image of permittivity distribution in 12 electrodes ECT sensor with 66 independent measurements is projected onto a (32x32) square pixel grid. On a (32x32) square pixel grid there are 1024 pixels, but only 812 pixels are needed to construct the cross-sectional image of the vessel [S. S. Donthi, 2004]. With 812 pixels, there are remaining pixels that are not being used because they are located outside the measurement area. The colour scale is used from blue to red that is “0” to “1” to indicate the range of the lower permittivity material to higher permittivity material.

In ECT, the capacitance of a parallel-plate capacitor constructed of two parallel plates both of area, A separated by a distance d is approximately equal to equation (5):

$$C = \frac{\epsilon_r \epsilon_0 A}{d} \quad \text{eq. (5)}$$

where,

C = the capacitance in farads, F

A = the area of overlap of the two plates measured in square metres

ϵ_r = the relative static permittivity of the material between the plates

ϵ_0 = the permittivity of free space where $\epsilon_0 = 8.854 \times 10^{-12}$ F/m

d = the separation between the plates, measured in metres.

One of the most commonly used reconstruction algorithm for image reconstruction in ECT system is the LBP because it is the simplest and fastest system for image reconstruction process. The LBP has been implemented to reconstruct images for ECT sensor using 12 electrodes and transducer-based multiprocessor system [B. Almashary, 2005]. With LBP, the permittivity distribution in ECT can be determined. The product of G is multiplication of the transpose of the transducer sensitivity matrix with the normalized capacitance matrix. The relationship can be seen in linear normalized form as in equation (6) [L. Yan, 2008]:

$$C = SG \quad \text{eq. (6)}$$

where,

C = the normalized capacitance matrix

S = the transducer sensitivity matrix which contains the set of sensitivity matrices for each electrode pairs

G = the normalized permittivity

2.9 The Differences between ECT and ERT

Basically, ECT and ERT have been developed separately as non-intrusive and/or non-invasive imaging techniques in the past [W. Q. Yang, 2004]. ECT can be used to visualise permittivity distributions while ERT is used to visualise conductivity distributions [W. Q. Yang, 2004]. Therefore, the ECT mode can be used to measure the dielectric component and ERT mode can be used to measure the conductive component. Both techniques that are stated before have their own advantages and disadvantages.

The differences and advantages, and disadvantages of ECT and ERT are shown in Table 4. The ERT measurement precision sometimes may be poor. Generally, in phase-flow, it has some strength compared to other techniques which are ERT can provides two or three

dimensional information on two-phase flow and phase distribution can be constructed various times. The advantages of ECT over other industrial tomography modalities are no radiation, fast imaging speed, non-intrusive and non-invasive, robust, withstanding high temperature and high pressure and of low cost [R. T. Atkins, 1998].

Table 4: Differences between ECT and ERT

ECT	ERT
Visualise permittivity distributions.	Visualise conductivity distributions.
Measure the dielectric component such as air, oil, or sand.	Measure the conductive component such as water acids bases and ionic solutions.
The advantages are no radiation, rapid response, low cost, non-intrusive and non-invasive.	Provide 2D and 3D flow, phase distribution can be constructed.
The disadvantage is issue of stray capacitance.	Low measurement precision but it is feasible to find precise method.

CHAPTER 3

METHODOLOGY

3.1 Research Methodology

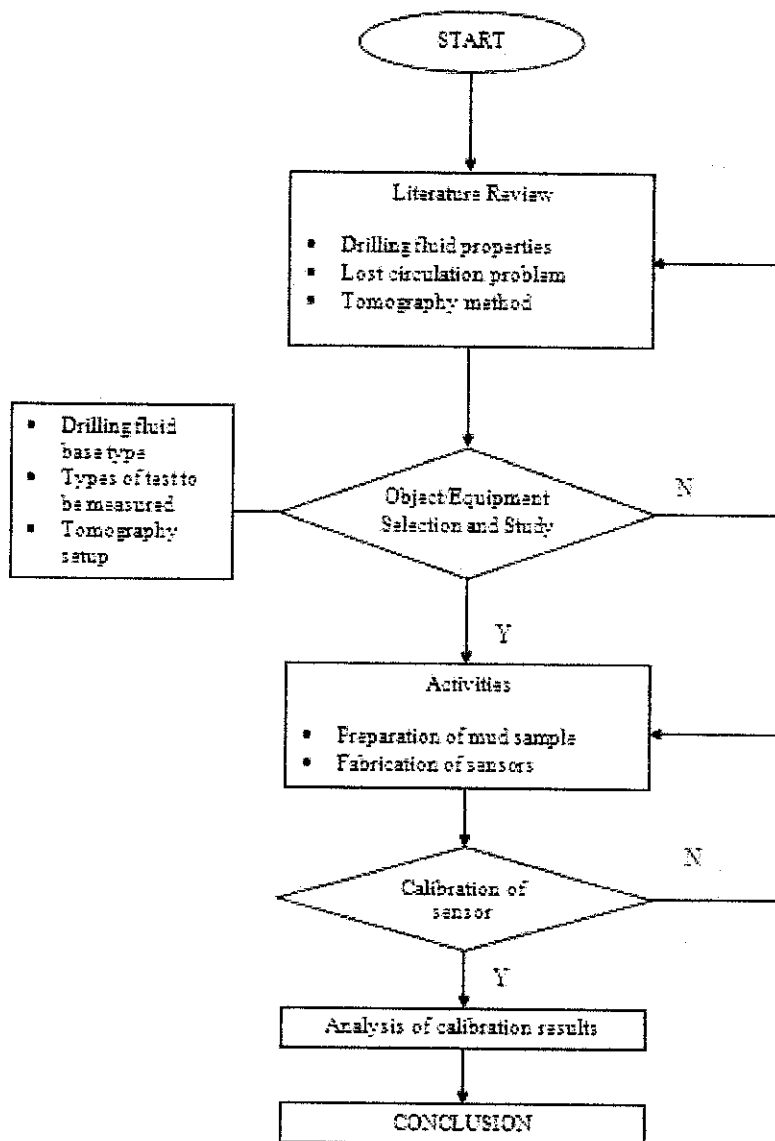


Figure 14: Project Methodology Process Flow

The project activities are referred to key milestones attached in Appendix E and G. The project is divided into five phases which are literature review phase, fabrication phase, testing phase, data analyzing phase and closure phase. Each phase consists of several tasks to be completed for Final Year Project. The first phase is done after the selection of the topic is made. In second phase, author discovered there is a possibility to develop new experimental set up to measure drilling fluid properties.

After analyzing on possibility of using tomography method to measure drilling fluid's properties, the ERT and ECT sensors are fabricated according to the design criteria. The third phase is the testing phase that includes the calibration measurement for ECT sensor testing. The fourth phase is the data analyzing phase which covers the data analyzing obtained from the testing phase. Finally, the last phase is the closure phase where the oral presentation is held. Figure 14 shows the project methodology process flow chart from the first until final phase.

3.2 Drilling Fluid Base Sample Preparation

The base sample is consists of water, soda ash as total hardness reducer, bentonite as viscosifier, flowzan or xanthan gum dispersible, barite as weighting agent and caustic soda as a pH modifier. The experiments are conducted in accordance with the standard stipulated in API RP 13B-1: Recommended Practice Standard Procedure for Field Testing Water-Based Drilling Fluids.

Flow chart



Procedures

- i. **0.5 ± 0.01 g** of **soda ash** was added into **318.73 ± 5 cm³** **deionized water** while stirring.
- ii. After **2 ± 0.5** minutes, a suspension of **75 μm** bentonite powder was prepared by adding **12 ± 0.01 g** of **bentonite** into the mixture while stirring.

- iii. After stirring for 7 ± 0.5 minutes, 0.3 ± 0.01 g of viscosifier or commercially known as **flowzan** was added into the mixture.
- iv. From time to time, remove the container from the mixer and scrape its side with the spatula to dislodge any bentonite adhering to the container walls. All bentonite clinging to the spatula are being assured to incorporate into the suspension.
- v. After stirring for 12 ± 0.5 minutes, 109.19 ± 0.01 g of **barite** was added into the mixture.
- vi. After 30 minutes, the **additive** was added into the mixture carefully.
- vii. Lastly, 0.25 ± 0.05 g of **caustic soda** was added into the mixture.
- viii. The container is then will be replaced and continued to stir. The container may need to be removed from the mixer and the sides scraped to dislodge any bentonite clinging to container walls after another 5 minutes therefore total stirring time is equal to 40 ± 1 minute.

3.3 Drilling Fluid Base Sample Weight Measurement

- i. Instrument base must be set on a flat level surface.
- ii. Measure and record the sample temperature.
- iii. Fill the mud cup with the sample to be tested.
- iv. Replace cap and rotate until it is firmly sealed, ensuring some of the sample is expelled through the hole on top, to free any trapped gas.
- v. Place the beam on the base support and balance it by using the rider along the graduated scale. Balance is achieved when the bubble is directly under the centre line.
- vi. Take the sample weight reading.



Figure 15: Multi-Mixer (left) and Mud Balance

3.4 Drilling Fluid Base Sample Rheology Test

In drilling fluid rheology testing, rheometer is used. It is important to frequently monitor the drilling fluid rheology as to make sure that the mud is always within the specification as stated in the mud program:

- i. Place the sample in the rheometer thermo cup and adjust the cup until the sample surface level is equal height to the scribed line on the rotor surface.
- ii. Turn on the rheometer, first taking dial measurements at the top most speed (600rpm), then gradually switch to lower gear and to obtain all readings (600,300,200,100,6,3rpms).

- i. **Determining PV** – indicate the amount of solids (sands, silts) in sample. High PV means that the sample is not clean and there is a problem with the solids control equipment.

$$PV = 600 \text{ rpm} - 300 \text{ rpm}$$

- ii. **Determining YP** – indicate the carrying capacity of cuttings (usually the case is that the higher the viscosity is, the higher the YP is)

$$YP = 300 \text{ rpm} - PV$$

- iii. **Determining Gel Value of the mud using Rheometer:**

- i. Stir the sample in 600rpm speed for 15 seconds. Just before the motor stops, slowly shift the moving gear to the lowest speed.
- ii. Wait for 10 seconds. After 10 seconds has finished, turn on the 3rpm speed and record the maximum deflection of the dial. This is the 10 seconds gel reading.
- iii. Repeat step one and step two, but this time, wait for 10 minutes before turning on the 3rpm speed. The maximum deflection of this reading shall give us the 10-minute gel reading.
- iv. Rewrite the gel value as (dial = 10 secs) / (dial = 10 mins)



Figure 16: Viscometer

3.5 ERT Sensor Design

In the ERT sensor design, 16-electrodes with 2 planes was fabricated. Specifications of the upper and lower plane are the same. The specifications of the sensor are in Table 5. Steps and procedures involved in the fabrication process are explained in the Table 6. Calibration measurement need to be run to ensure the sensor is functioning.



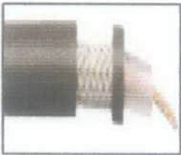

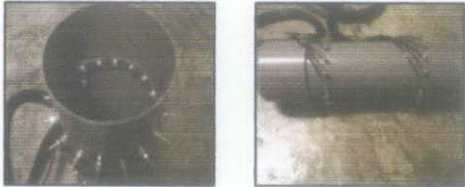

Table 5: ERT Sensor Specification for 1 plane

No	ECT sensor components	Specifications
1	Number of electrodes	16
2	Electrodes length	1.50 cm
3	Electrodes width	1.50 cm
4	Electrode thickness	0.05 cm
5	Distance between electrodes	0.30 cm
6	Inner PVC diameter	8.60 cm
7	Outer PVC diameter	9.00 cm

To measure distance between electrodes :

$$\frac{\text{Electrode Diameter}}{\text{Inter-Electrode Gap}} = \frac{1.5}{5} = 0.3 \text{ cm}$$

Table 6: ERT Sensor Fabrication Steps

No	Steps	Remarks
1	<p>Material of sensor is selected</p> <ul style="list-style-type: none"> I. Body– Polyvinyl chloride (PVC) Pipe II. Electrode– Zinc III. Coaxial Data Cable IV. Centronic Plug 	<p>I. </p> <p>II. </p> <p>III. </p> <p>IV. </p>
2	<p>Specification of the sensor and arrangement of the electrodes are determined. There is a ground electrode below each of the measurement electrodes plane.</p>	<p>Refer to Table 5</p>
3	<p>Electrodes are arranged and drilled uniformly around circumference of column. Electrodes must be able to make contact with the sample within the process volume.</p>	
4	<p>The electrodes' sensor are connected to the Data Acquisition System (DAQ) using coaxial data cable terminated with the centronic plugs.</p>	

3.6 ECT Sensor Design



In the ECT sensor design, 12 electrodes with only one plane was fabricated. In order to fabricate the sensor, the steps are quite similar with ERT sensor fabrication.


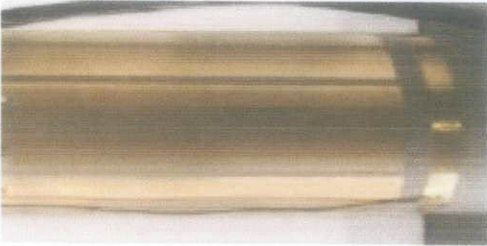

Table 7: ECT Sensor Specification

No	ECT sensor components	Specifications
1	Number of electrodes	12
2	Electrodes length	15.00 cm
3	Electrodes width	2.00 cm
4	Ground electrode width	1.00 cm
5	Distance between electrodes	0.33 cm
6	Inner PVC diameter	8.60 cm
7	Outer PVC diameter	9.00 cm

Table 7 shows the specification lists of the ECT sensor that includes the number of electrodes, electrodes length, electrodes width, distance between two measurement electrodes, ground electrode width, inner and outer diameter of PVC. In Table 8, it shows the steps involve in fabricating the ECT sensor. The fabrication consists of several portions such as the data cable, SMB plug, and the electrodes. Soldering technique was used to assemble most of the portion of the sensor.

Table 8: ECT Sensor Fabrication Steps

No	Steps	Remarks
1	<p>Prepare the data cable with the SMB plug. The steps are:</p> <ol style="list-style-type: none"> I. Gather the SMB plug portion II. Solder the SMB plug needle with the gold multi core wire in the data cable. III. Assemble the SMB plug with the data cable. 	<p>I.</p>  <p>II.</p> 

		<p>III.</p> 
2	<p>Measure the PVC diameter and decide the length of the electrodes. Place the copper tape on the PVC. There is a ground electrode on top of the measurement electrodes plane.</p>	
3	<p>From the data cable, mount the silver multi core wire at the ground or earth electrodes portion while the gold multi core wire at the electrodes portion.</p>	

CHAPTER 4

RESULTS AND DISCUSSION

4.1 Drilling Fluid Base Sample Rheology Test

The experiments were conducted according to the standard which has stipulated in American Petroleum Institute – API 13B-1; ‘Recommended Practice Standard Procedure for Testing Water-Based Drilling Fluid’. In the experiment, the mud was mixed with additives as suggested by the API 13B-1 such as bentonite, and any changes of the properties were observed. Figure 10 shows the composition of the drilling fluid base used in the experiment and Table 9 shows the properties of drilling fluid tested is at the concentration of 10 lb/bbl.

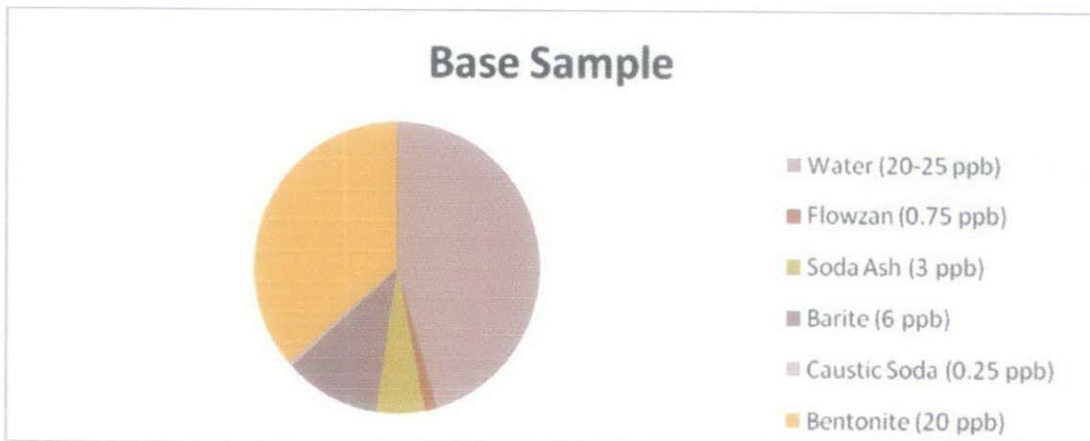


Figure 17: Drilling Fluid Base Sample Composition

Table 9: Properties of Drilling Fluid Base Sample at 10 lb/bbl

Mud Weight (ppg)	Rheology at 120 F (rpm/ppg)						PV (cP)	YP (lb/100ft ²)	Gel Strength (lb/100ft ²)		Mud Thickness (mm)	API (cc/30min)
	600	300	200	100	6	3			10secs	10mins		
									7	13		
10.5	45	32	26	20	9	8	13	19	7	13	1	19

The drilling fluid base sample tested is considered accepted by referring to the mud weight achieved [Scomi Oil]. The drilling fluid additives efficiency performance for LCM can be measured through plugging test. This test can be made by using High Temperature High Pressure (HTHP) Filter Press equipment with ceramic or metal slotted disc. This testing equipment is available in UTP laboratory. The problem occurs when the ceramic and metal slotted disc is not available.



Figure 18: Filter Press Drilling Fluid Testing Equipment

To make the results more variable and comprehensible, a test rig has been planned be developed.

4.2 Filtration Test Rig Design

The design of the test rig is still in early stage. The preliminary design was done by using Autodesk Inventor Professional 2010 software.

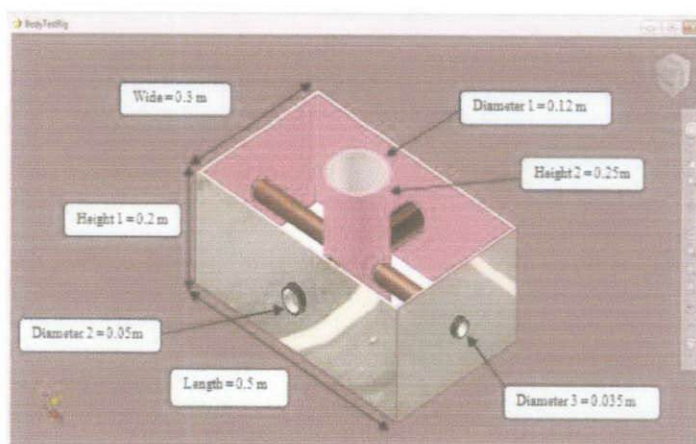


Figure 19: Design of Test Rig Body

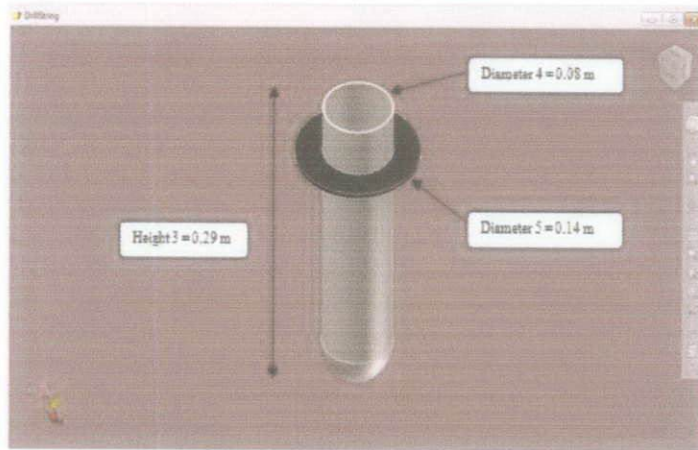


Figure 20: Design of Test Rig Drill String

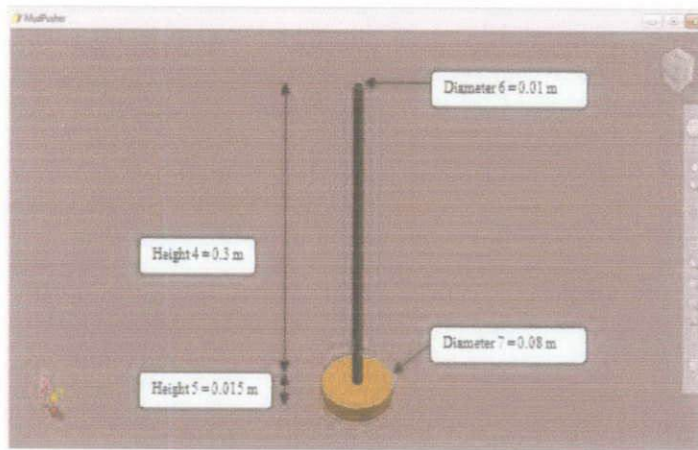


Figure 21: Design of Test Rig Mud Pusher

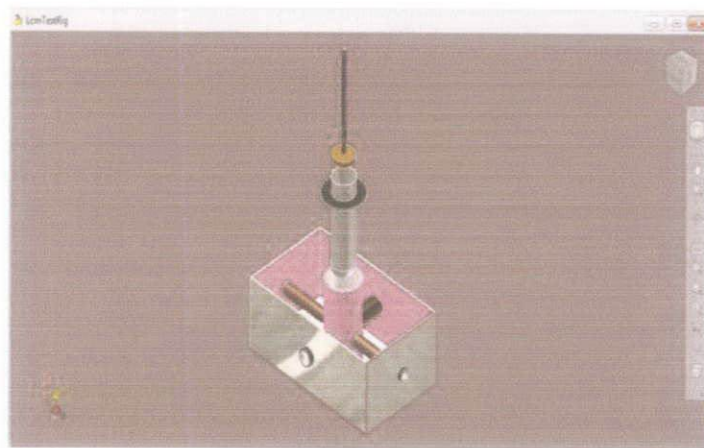


Figure 22: Assembly Drawing of Test Rig

The objective of the test rig is to study the filtration properties of the drilling fluid. However, there are more parameters that needs to be included in the consideration such as temperature, pressure, stress and material analysis. After research and study analysis about the test rig has been done, the development cannot be continued when the author discovered that a lot of assumptions have to be made making the rig condition too ideal and unrealistic.

The author later then explored the possibilities of using the tomography method to be used in measuring the drilling fluid properties. The study started by searching the applications of tomography method in oil and gas specially for drilling fluid purposes. The tomography method focused on ERT and ECT concepts. Both of the sensors have been fabricated and the calibration test measurement has been done on ECT sensor.

4.3 Calibration Measurement of ECT sensor

The calibration was conducted by connecting the SMB plugs of 12 electrodes on the ECT sensor to the CTPI plane of ITS device. The calibration procedure starts with the calibration of lower permittivity material that is dry air and continued with higher permittivity material that is water. During the calibration measurement, the raw capacitance value for 66 independent capacitance measurements is recorded by ITS software. The calculation of independent capacitance measurements value is by using equation $N(N-1)/2$, where N is the number of electrodes. Figure 23 shows the calibration setup while figure 24 shows that the color scale of low and high calibration is differ from blue to red that is indicating '0' for low (blue) and '1' for high (red).

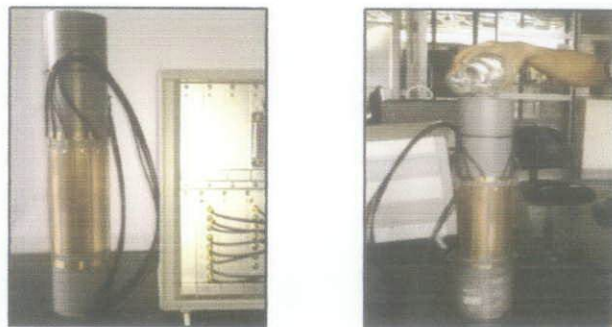
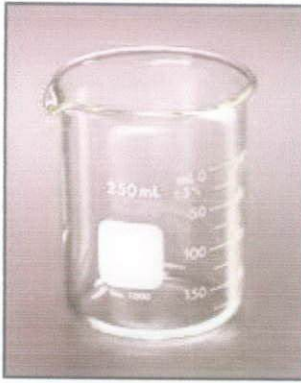
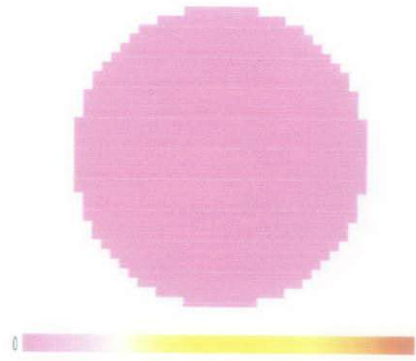


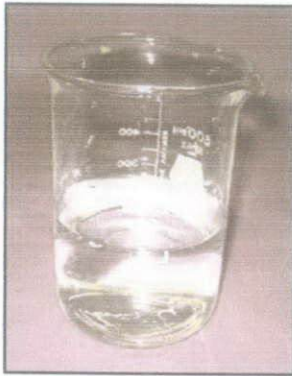
Figure 23: Calibration Setup



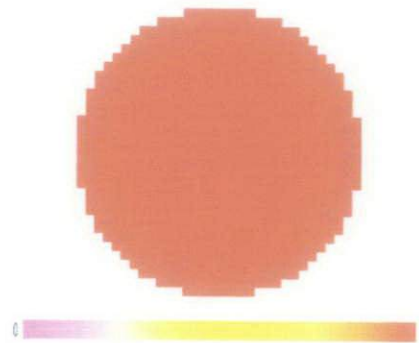
Dry Air



Low Calibration



Water



High Calibration

Figure 24: Low and High Calibration Images

4.4 Measurement Results

After doing the calibration measurement test, the online measurement was done using the drilling fluid base sample. The online measurement is referring to the sample other than calibration's sample. From the experimental setup, the sensor transmitted the reading while the data acquisition system recorded and transferred to the software in the computer to be processed. There are more than 10 types of output can be processed by the Industrial Tomography Systems (ITS) software such as the images of material capacitance and permittivity, the raw capacitance value and the value of material's voltage. Figure 25 shows the image of drilling fluid base sample permittivity.

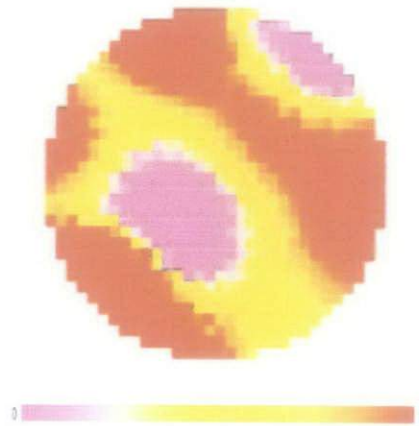


Figure 25: Image of Drilling Fluid Base Sample in Online Measurement

Table 10 shows the voltage values recorded between each pair of the electrode in the sensor. There are 12 electrodes which results in 66 different pairs and values. During the measurement, voltage is applied to single electrode then the voltage differences at other electrode are measured. Important principle during the measurement of ECT is when 1 pair of electrode is being measured, other electrodes will act as ground. Table 10 just shows 11 values of voltage measurement from 11 differences pairs.

Table 10: Voltage Values Measurement

	ELECTRODE PAIRS (VOLTAGE)										
	E1-E2	E1-E3	E1-E4	E1-E5	E1-E6	E1-E7	E1-E8	E1-E9	E1-E10	E1-E11	E1-E12
LOW	1366.18	725.397	667.567	653.282	646.169	648.077	648.672	666.27	683.028	730.601	1367.05
	1366.18	725.397	667.567	653.282	646.169	648.077	648.672	666.27	683.028	730.601	1367.05
HIGH	1063.89	768.514	756.655	750.092	645.955	738.584	743.605	755.113	767.582	772.802	1064.03
	1063.31	767.521	755.846	749.161	645.742	737.622	742.811	754.289	766.667	771.917	1064.87
ONLINE	1348.93	750.488	685.028	665.202	646.139	656.426	657.967	675.931	699.42	756.395	1347.39
	1348.87	750.58	685.043	665.186	646.352	656.365	658.013	675.855	699.329	756.166	1347.61

The graph of the voltage measurement value versus the number of measurement was plotted as figure 26. The graph combines three materials which are dry air for low calibration, water for high calibration and drilling fluid base sample for online measurement. All the 66 electrode pairs voltage measurement value were included to show the overall pattern of each material.

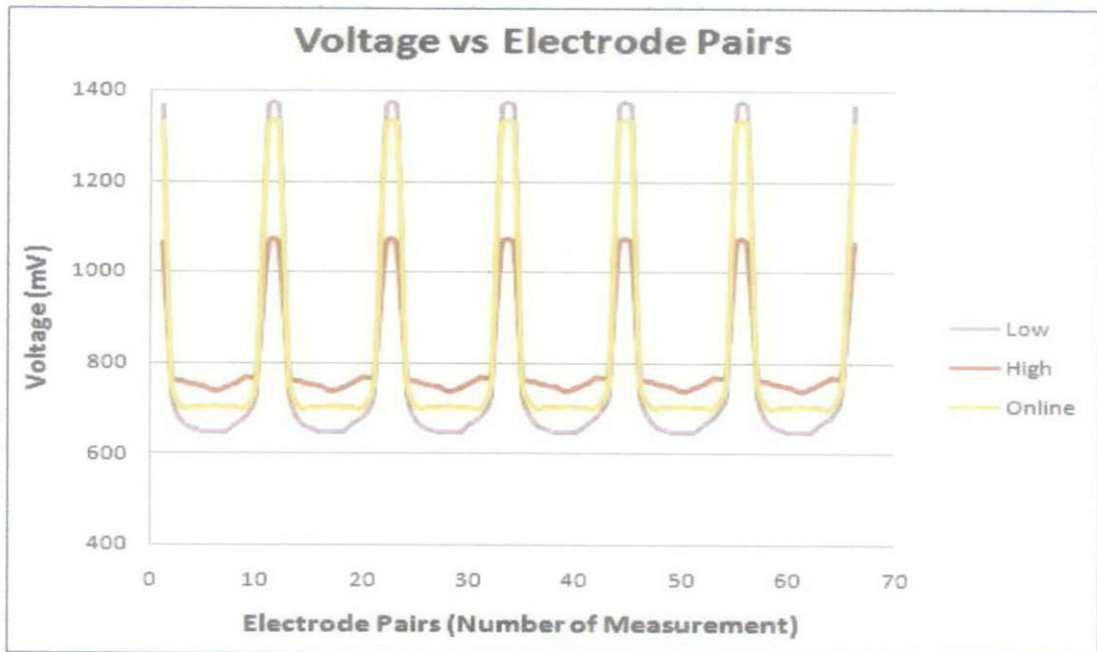


Figure 26: Voltage vs. Electrode Pairs

4.5 Discussion

The drilling fluid base sample is set for the purpose of comparison before the usage of additives into the mud formulation. It consists of water, soda ash as total hardness reducer, bentonite as viscosifier, flowzan or xanthan gum dispersible, barite as weighting agent and caustic soda as a pH modifier. To fulfill the function of LCM, one the physical properties of the additive is a fiber. Oil palm empty fruit bunch has been used in this experiment. An example of LCM additive than being use currently in the industry is nut hulls.

The experiments were conducted in accordance with the standard stipulated in API RP 13B-1: Recommended Practice Standard Procedure for Field Testing Water-Based Drilling Fluids. In the experiment, the mud was mixed with additives as suggested by the API 13B-1 such as bentonite, and any changes of the properties were observed.

To get a good LCM, filtration properties need to be measured. Filtrates are the liquid part of the mud. When the mud is forced against a permeable zone, the solids in the mud will

form a plaster or “wall cake” against the formation face. Some of the liquid fraction will filter through this cake and into the formation. This liquid fraction (water plus dissolved salts) is the filtrate. Due to the unavailable test equipment, the test cannot be done.

The author then study the possibilities of using the tomography method to measure LCM properties. Under the separation application, there is a possibility to measure the filtration properties. Before going to the filtration, drilling fluid’s conductivity and permittivity are the primary properties of interest because they determine the impedance of drilling fluid standoff layer. Conductivity is related to resistance while permittivity is related to the capacitance. To measure conductivity, ERT sensor can be use. The replica sensor has been fabricated but the test measurement cannot be done because the malfunction of ERT electrode panel at the M3000 Multi-Modal Data Acquisition Unit.

Referring to the need of measuring permittivity, ECT replica sensor also has been fabricated. From the test calibration and online measurements, the results of material’s permittivity images were obtained. ECT systems are based on a linear relationship between capacitance and permittivity values. The lower capacitance material will have lower permittivity. In relation with that, the lower permittivity material will have higher voltage measurement (VMS). Greater difference in permittivity values will produce larger difference in voltage measurement.

Overall, there are 11 steps in the experimental setup to measure conductivity or permittivity using tomography method.

- i. ERT sensor is filled with water (skip this step for ECT measurement)
- ii. Connect sensor to Data Acquisition Unit via 36 way Centronics
- iii. Connect adapter power lead to the system
- iv. Switch the front panel 'Grey' button (red light)
- v. Switch the sensor power on (back panel)-blinking light at front panel
- vi. Open Multi-Modal Tomography Configuration (MMTC)

- vii. Open file (e.g. 'ERT-onep-1')
- viii. Change 'ERT/ECT Cal' in the flow chart window to low (0)
- ix. Change 'Write ERT/ECT' in the flow chart window to multiple frame '0'
- x. Click 'RUN' to get the measurement data
- xi. Repeat from STEP 5 for 'ERT/ECT Cal' in high (1) then change to None (2)

Above steps are applicable for both static and dynamic test measurements. Dynamic test will give better results in term of representing the real situation application. Last but not least, further analysis need to be done to calculated the permittivity and impedance values.

CHAPTER 5

CONCLUSION AND RECOMMENDATION

5.1 Conclusion

In the drilling operation, drilling fluid is one of the most important aspects that need to be taken care of carefully. The study of drilling fluid properties is the basic in understanding of the drilling fluid applications either for onshore or offshore operation. The progression of drilling operation is always unexpected, for this reason the drilling fluid or mud engineer need to be ready each time there is a need to change the drilling fluid program being used. Lost circulation is one of the most serious and expensive problems in the drilling operation. To solve this problem, the drilling fluid used need to have a capability to seal the fractures by plugging them.

In order to develop the experimental setup of evaluating the drilling fluid's properties using tomography method, the ERT sensor has been fabricated. Due to the malfunction of data acquisition unit, the measurement using the sensor cannot be done. Hence, the ECT sensor has been fabricated which consists of measurement electrodes, earth screen at both ends of measurement electrodes and shielding to avoid direct contact with the measuring medium. The measurement electrodes are located outside the insulating pipe to prevent from direct contact with the material inside the insulating pipe. Moreover, the earth screen is used to avoid interferences between the sensor's applied signal and any devices present near the sensor. 12 measurement electrodes are chosen in order to obtain more independent capacitance measurement that is 66 measurements.

The calibration of the sensor includes low and high calibration which is conducted by using lowest and highest permittivity material. Dry air is being used for low calibration while water is used for high calibration. The mixture of water in the material affects the permittivity value of the material. In an online measurement, the drilling fluid base

sample has been used. The test is in static condition and the analysis is based on the voltage measured between the electrode pairs. The lower permittivity material will have higher voltage than the higher permittivity material. The images captured by the sensor only show the ratio of the capacitance and permittivity of the material. Further analysis and calculation need to be done to measure the exact values of the properties.

As a conclusion, the development of the experimental setup to evaluate the drilling fluid's characteristic using the tomography method shows that it has high potential to go further. Current results and analysis is not strong enough to be set as a final result but it can be used as a basis to evaluate desired properties such as the filtration in case of LCM. Nevertheless, this experimental setup is also meant to evaluate other types of drilling fluid.

5.2 Recommendation

For future work development, the ERT sensor calibration test measurement should be carried out since the sensor replica has been fabricated. The measurement of the material can be done through the steps that have been developed. From the injected current to the electrode's sensor, the voltage and resistance can be calculated to evaluate the drilling fluid's properties.

The calibration and online measurement has been done using ECT sensor. There is a need to enhance the technique of evaluating the current results and analysis to get other properties such as material's permittivity values. The connection and relationship between other properties will also help in measuring the filtration properties.

For the initial starting procedure, the calibration and online measurement usually started with static analysis. To get more comprehensive and real situation application results, it is important to conduct dynamic analysis for both ECT and ERT sensor measurement. Development of test rig or flow loop might be a good procedure to evaluate the drilling fluid in dynamic analysis.

REFERENCES

- 1 Amanullah M (1993). Shale-drilling mud interactions, PhD thesis, University of London ; 275.
- 2 Amanullah M, Yu L (2005). "Environment friendly fluid loss additives to protect the marine environment from the detrimental effect of mud additives", *Journal of Petroleum Science and Engineering* ; 48(3-4):199-208.
- 3 Aminuddin, M. (2006). "*Performance of Ester-Internal Olefin Based Drilling Fluid*", Universiti Teknologi Petronas.
- 4 Azuraieen Jaafar (2010). Class Lecture Notes, University Technology of PETRONAS.
- 5 Baharuddin Mohamed Haris (2010). Drilling fluid consultant for Petro Canada Libya.
- 6 B. Almashary, S. M. Qasim, S. Alshebeili, and W. A. Al-Masry (2005). "Realization of Linear Back-Projection Algorithm for Capacitance Tomography Using FPGA," 4th World Congress on Industrial Process Tomography ; 88-93
- 7 Drilling Engineering Manual (2010). Department of Petroleum Engineering, Curtin University of Technology.
- 8 Drilling mud and cement slurry rheology manual (1982). Paris, Technip Editions.
- 9 D. A. Robinson, C. M. K. Gardner, J. Evans, J. D. Cooper. M. G Hodnett, and J. P Bell (1998). "The dielectric calibration of capacitance probe for soil hydrology using an oscillation frequency response model," *Hydrology and Earth System Sciences*, 2(1), pp. 111-20.
- 10 F. L. Quak (2008). Electrical Resistance Tomography. Department of Chemical and Biological Engineering University of British Columbia.
- 11 F. Ulaby (2005). *Electromagnetics for Engineers*. NJ: Pearson Education Inc. 2005, pp. 99.
- 12 K.J Alme, S.Mylvaganam (2006). Analyzing 3D and Conductivity Effects in Electrical Liesman S, Big oil starts to tap vast reserves buried far below the waves, *Wall Street Journal*, 3 July 2000.

- 13 L. Yan, B. Peiquan, C. Peng, F. Li, and Z. Liyong (2008). "A New Image Reconstruction Algorithm for Electrical Capacitance Tomography," 11th Joint Conference on Information Sciences, pp.1-6.
- 14 McKee et al. (1995). "A New Development Towards Improved Synthetic-Based Mud Performance". SPE/IADC Drilling Conference in Amsterdam, 28 Feb-March 1995. Amsterdam SPE/IADC 29405 (235-237).
- 15 Oil online, Glossary of Terms.
- 16 Process Tomography Ltd./ Tomoflow Ltd. "Electrical Capacitance Tomography," 2004.<http://www.tomography.com/pdf/ectfund.pdf>.
- 17 Reid PI, Elliot GP, Milton RC, Burt DA (7-10 March 1993). "Reduced environmental effect and improved drilling performance with water-based muds containing glycols". SPE/EPA Exploration and Production Environmental Conference, San Antonio, Texas, SPE 25989, 453-63.
- 18 R. Giguere, L.Fradette, D.Mignon and P.A. Tanguy (2007). ERT algorithms for quantitative concentration measurement of multiphase flows.
- 19 R. T. Atkins, T. Pangburn, R. E. Bates, and B. E. Brockett (1998). "Soil Moisture Determinations Using Capacitance Probe Methodology," Cold Regions Research & Engineering Laboratory, US Army Corps of Engineers, Special Report 98-2.
- 20 S. M. Huang, C. G. Xie, R. Thorn, D. Snowden, and M. S. Beck (1992). "Design of sensor electronics for electrical capacitance tomography" IEE Proc. G 139, pp. 83-8.
- 21 S. S. Donthi (2004). "Capacitance based Tomography for Industrial Applications," M. Tech Electronics Systems Group, EE Dept, IIT Bombay, pp. 1-18.
- 22 Telford, W.M., L.P. Geldart, R.E. Sheriff (1990). Applied geophysics. 2nd ed. Cambridge Univ. Press, Cambridge, UK.
- 23 Van Dyke, Kate (1951). *Drilling fluids –Rotary drilling series*; unit II, lesson 2, ISBN 0-88698-189-1.
- 24 W. Q. Yang, A Chondronasios, S. Nattrass, V. T. Nyuyen, M. Betting, I. Ismail, and H. McCann (2004). "Adaptive calibration of a capacitance tomography system for imaging water droplet distribution", Flow Measurement and Instrumentation, pp. 249-258.

- 25 W. Q. Yang (2010). "Design of electrical capacitance tomography sensors", Meas. Sci. Technol, pp. 13.
- 26 Z.Z. Yu, A.J, M.S Beck (1995). Optimum Excitation Field for Non-intrusive Electrical and Magnetic Tomographic Sensor. Process Tomography Group.

APPENDIX A

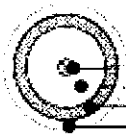
DATA CABLE

	TECHNICAL DATA SHEET	code	MRC1740
		version	2
		date	2008-11-09
	R.F. CABLE 50 OHM RG-174 U CCS	page	1/2

APPLICATION

Coaxial cable used for Radio-frequency, designed according MIL-C-174 U19F

CONSTRUCTION



1. Conductor
2. Dielectric
3. Screen
4. Sheath

1) Conductor	7x0.16 mm copper clad steel wire
Diameter	0.5 mm
2) Dielectric	Solid PE
Diameter	1.50 mm = 0.10 mm
3) Screen	braid
Material	0.1 mm tinned copper wire
Diameter	1.97 mm = 0.11 mm
4) Sheath	PVC
Diameter	2.80 mm = 0.10 mm
Color	black

REQUIREMENTS AND TEST METHODS

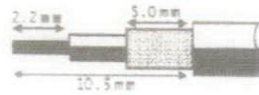
Test methods generally in accordance with MIL-C-174 U19F

1) Conductor	
Elongation at break	≥ 10%
2) Screen	
Coverage	88 %

Electrical characteristics

Mean characteristic impedance	50 ± 2 Ohm	
DC resistance inner conductor	≤ 317 Ohm/km	
Capacitance at 1 kHz	100 ± 3 pF/m	
Velocity ratio	0.66 ± 0.02	
Insulation resistance	≥ 10 ⁶ MOhm.km	
Voltage test of dielectric	3 kV dc	
Corona	≤ 1.5 kV ac	
Return loss at:	100 – 400 MHz	≥ 22.5 dB
	400 – 600 MHz	≥ 19.2 dB

APPENDIX B
STRAIGHT FEMALE CRIMP PLUG



Attributes

Attribute Type	Attribute Value
Gender	Jack
Mounting	cable
Orientation	Straight
Impedance Ω	50
Contact Plating	Gold
Contact Material	beryllium copper
Contact Termination Method	Solder
Cable Type	RG174A/U

Range Overview

SMB 50 Ω Connectors in clamp and crimp termination options.
Reliable and quick connect/ disconnect system

Technical specification	
Working Voltage	250V max.
Proof Voltage	750V rms max.
Insulation Resistance	$> 5 \times 10^9 \Omega$
Temperature Range	-65°C to +165°C

APPENDIX C

COPPER FOIL SHIELDING TAPE

Technical Data

Issue 2 / July 2006

AT526 35 Micron Copper Foil Shielding Tape

General description

35 micron copper foil coated with an electrically conductive acrylic adhesive supplied on a removable silicone liner.

- Conductive acrylic adhesive
- Good high and low temperature resistance
- Can be easily soldered
- Easy unwind

Specification

- Tested in accordance with ASTM D-1000 latest issue, BS EN 60454 - Part 2 test methods (Formerly VDE 0340, BS 3924.)
- Tested and meets military specification MIL - T - 47012
- Construction is tested in-house and conforms to the Flame retardant requirement part only of UL510

Technical Details

Technical details	BS value	ASTM value
Typical values		
Foil thickness:	0.035mm	1.4 mil
Adhesive thickness:	0.025mm	1.0 mil
Total thickness:	0.060mm	2.4 mil
Adhesion to steel:	4.5 N/cm	41 oz/inch
Tensile strength:	40 N/cm	23 lbs/inch
Temperature Resistance:	-20°C to +155°C	Up to +311°F
Recommended curing cycle:	1 hour at 150°C or 2 hours at 130°C	
Electrical resistance through		
Adhesive*:	0.003 ohms	
RoHS compliant:	Yes	
Storage Temperature:	-12°C to +25°C	

* Tested according to MIL STD 202F method 307 across surface area of 1 sq inch.



NOTE

Except where indicated otherwise, all figures stated are either typical values and should not be regarded as MAXIMUM or MINIMUM values for specification purposes. The Company reserves the right to improve products and any change in specification will result in a re-issue of the relevant Technical Data Sheet. Customers should satisfy themselves that the tape is suitable for their requirements whether with their manufacturers or otherwise. Please check that you have the latest issue of the Technical Data Sheet. An ordering and shipping instruction slip is printed on the back of the customer's order to assist in completing the Order-A Safety Data Sheet produced by the company for this product, which is available on request.

STORAGE

Tapes should be stored at the minimum recommended temperature and require warming up to the use temperature. Up to 24 hours may be required for this to take place.

 **ADVANCE**
adhesive tapes

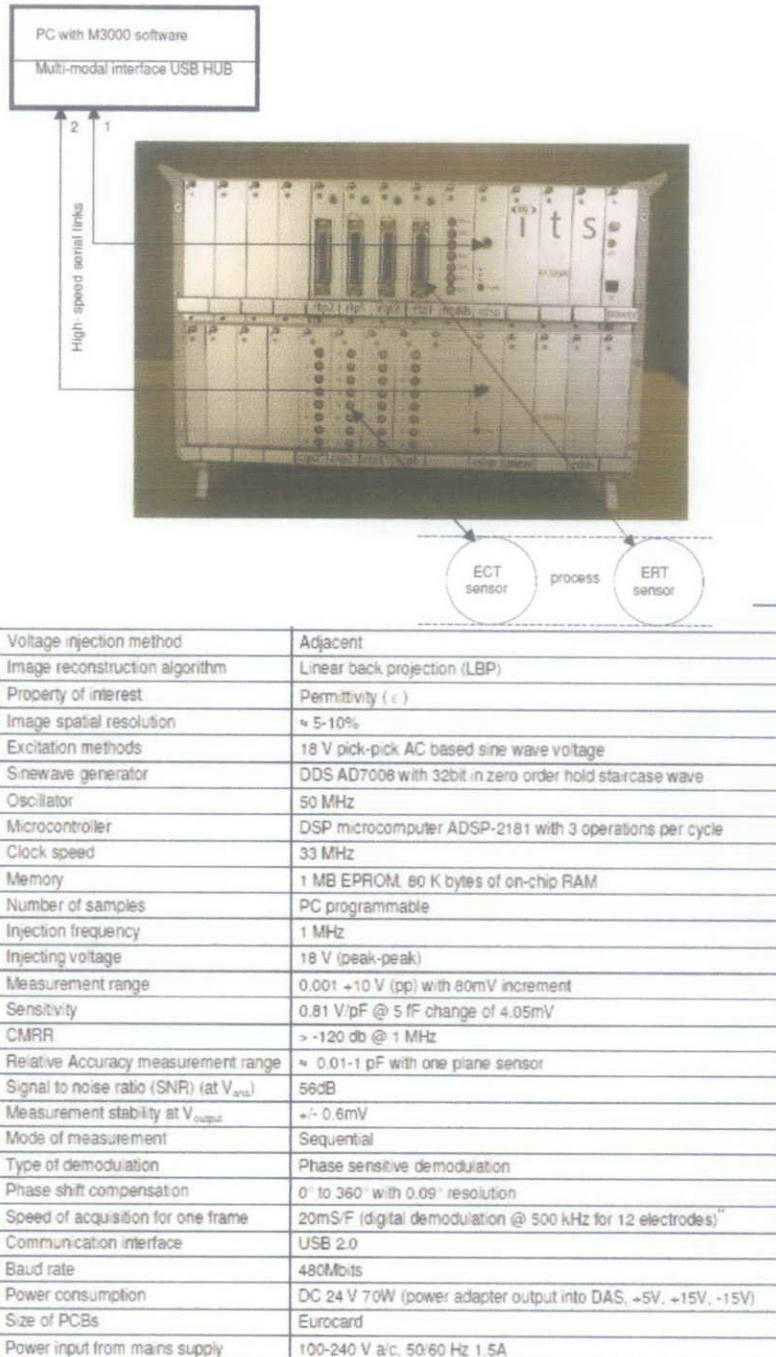


Advance Tapes International Limited, PO Box 122,
Abbey Meadows, Leicester, LE4 5RA.
Tel: 0116 251 0191. Fax: 0116 265 2046. www.advancetapes.com

AFERA
Association des Fabricants Européens de
Rubans Auto-Adhésifs.

APPENDIX D

INDUSTRIAL TOMOGRAPHY SYSTEM DEVICE



Appendix E: Key Milestone for FYP 1

Suggested Milestone for Final Year Project I

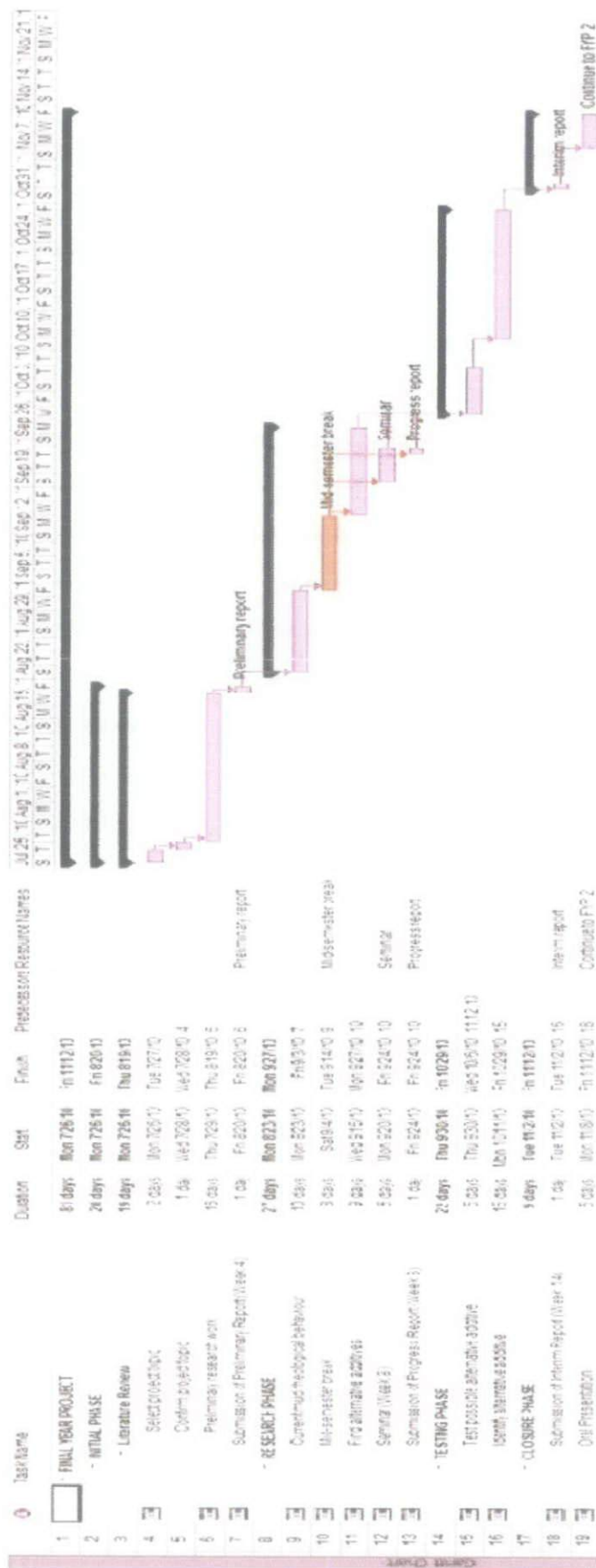
No	Detail/Week	1	2	3	4	5	6	Mid-semester break				7	8	9	10	11	12	13	14	
1	Selection of Project Topic	█																		
2	Preliminary Research Work		█	█																
3	Submission of Preliminary Report				●															
4	Project Work					█	█													
5	Submission of Progress Report												●							
6	Seminar (compulsory)												●							
7	Project work continues													█	█	█	█	█	█	█
8	Submission of Interim Report Final Draft																			●
9	Oral Presentation																			

● Suggested milestone

█ Process

During study week

Appendix F: Gantt chart



Appendix G: Key Milestone for FYP 2

Suggested Milestone for Final Year Project II

No	Detail/Week	1	2	3	4	5	6	Mid-semester break							7	8	9	10	11	12	13	14
1	Project work continues																					
2	Submission of Progress Report 1				●																	
3	Project work continues																					
4	Submission of Progress Report 2																					
5	Seminar (compulsory)																					
6	Project work continues																					
7	Poster Exhibition																					
8	Submission of Dissertation Final Draft																					
9	Oral Presentation																					
10	Submission of Dissertation (hard bound)																					

● Suggested milestone

■ Process

During study week

7 days after oral presentation